REPORT DOCUMENTATION PAGE

AFRL-SR-AR-TR-06-0072

1. REPORT DATE *(DD-MM-YYYY)*	2. REPORT TYPE	3. DATES COVERED *(From - To)*
03/07/2006	Final	1 March 2005 - 28 February 2006

4. TITLE AND SUBTITLE
Delivery of MISAR Algorithms

5a. CONTRACT NUMBER

5b. GRANT NUMBER
FA9550-05-C-0029

5c. PROGRAM ELEMENT NUMBER

6. AUTHOR(S)
Richard Tolimieri

5d. PROJECT NUMBER

5e. TASK NUMBER

5f. WORK UNIT NUMBER

7. PERFORMING ORGANIZATION NAME(S) AND ADDRESS(ES)
Promethus Inc.
103 Mansfield Street
Sharon, MA 02067

8. PERFORMING ORGANIZATION REPORT NUMBER

9. SPONSORING/MONITORING AGENCY NAME(S) AND ADDRESS(ES)
Air Force Office of Scientific Research
875 N. Randolph Street, Suite 325, Room 3112
Arlington, VA 22203-1768

10. SPONSOR/MONITOR'S ACRONYM(S)
AFOSR

11. SPONSOR/MONITOR'S REPORT NUMBER(S)

12. DISTRIBUTION/AVAILABILITY STATEMENT
Distribution Statement A. Approved for public release; distribution is unlimited.

13. SUPPLEMENTARY NOTES

14. ABSTRACT
In parallel with these applications we develop several topics in the theory of the finite Zak transform (FZT). The FZT maps one-dimensional signals (vectors) onto two-dimensional signals (matrices). The Zak space representation provides a time-frequency image of the one-dimensional signal. Signal decomposition and processing such as convolution, matched filtering and the Fourier transform can be interpreted geometrically and computed by matrix operations in Zak space.

15. SUBJECT TERMS

16. SECURITY CLASSIFICATION OF:			17. LIMITATION OF ABSTRACT	18. NUMBER OF PAGES	19a. NAME OF RESPONSIBLE PERSON
a. REPORT	b. ABSTRACT	c. THIS PAGE			Richard Tolimieri
U	U	U	UU		19b. TELEPHONE NUMBER *(Include area code)* 401-849-5389

Final Executive Summary

7 March 2006

Sponsored by
Air Force Office of Scientific Research
USAF, AFRL

Contract # FA9550-05-C-0029

Contractor: Prometheus Inc.
Business Address: 103 Mansfield Street, Sharon, MA 02067

Effective Date of Contract: 01 March 2005
Contract Expiration Date: 28 February 2006
Reporting Period: 01 March 2005 – 28 February 2006

Principal Investigator: Richard Tolimieri
Phone Number: (401) 849-5389, (781) 784-2355

Title: Delivery of MISAR Algorithms

Authors: Richard Tolimieri, Myoung An

1 Introduction

The two applications addressed in this report are

- spatial localization and scattering coefficient computation from the noisy echoes of chirp pulses interrogating a multiple point target environment,
- numerical deconvolution of Krueger's formula relating the reflectivity kernel ρ of a dielectric material to the echo resulting from the interaction of an orthogonally incident chirp pulse with the material.

In parallel with these applications we develop several topics in the theory of the finite Zak transform (FZT). The FZT maps one-dimensional signals (vectors) onto two-dimensional signals (matrices). The Zak space representation provides a time-frequency image of the one-dimensional signal. Signal decomposition and processing such as convolution, matched filtering and the Fourier transform can be interpreted geometrically and computed by matrix operations in Zak space.

A key feature in the Zak space approach not available in a standard time-domain or frequency-domain representation is that digital signal processing can be viewed through different time-frequency windows. For applications addressed in this report a specific window W_0 is taken, but windows can be chosen to match classes of waveforms, special signal decomposition and processing and application noise characteristics.

The physical model in the applications is the transmission of a chirp pulse and the critical sampling of its echo from a multiple point target environment or a dielectric material. We show that the collection of shifts of a critically sampled chirp pulse is orthogonal when viewed through the window W_0. A negative result of windowing is aliasing which will be discussed in detail, but for the present discussion will be ignored.

Through W_0 a critically sampled echo of a chirp pulse can be represented as an orthogonal linear expansion whose coefficients in the first application are the scattering coefficients of the targets and in the second application are samples of the reflectivity kernel. Matched filtering reduces to computing the coefficients of an orthogonal expansion.

A closely related, equally important result is that the *longer* the time duration of the chirp pulse, the finer its critical samples resolve targets and sample reflectivity kernels.

The FZT is especially tuned for chirp pulses. The main result here is that the support of the FZT of a critically sampled chirp pulse and its shifts are lines in W_0. The support of a critically sampled echo is a series of lines. Dechirping results in a series of horizontal lines.

Under certain conditions the windowed Zak space representation of a critically sampled echo of a chirp pulse can be image processed to reduce noise and clutter. This processing can stand alone or be a preprocessing step to the windowed matched filter approach described above.

As we will see these conditions place constraints on the number and/or values on the lines in the Zak space representation of the critically sampled echo. Essential use is also made of the vanishing off of these lines in the noise-free case.

The conditions under which these image processing methods apply are discussed mainly in Sections 6 and 14. In the first application the relationship between the product of the

chirp time duration and chirp rate and the number and/or spacing of targets is key. In the second application the relative sizes of the chirp time duration and the material relaxation time is the crucial factor.

In future work we expect to extend these results to multiple chirp and chirp pulse train interrogation of a multiple target scene consisting of point scatterers, perhaps in motion, and dielectric scatterers. Chirp parameters, time-duration, chirp rate and carrier frequencies may vary over the application.

A second future goal is to develop the FZT into a waveform design tool. Based on the work in this report, we expect to design discrete waveforms directly in Zak space exploiting the relationship between the geometric structures supporting these waveforms in Zak space and the effect of linear shifts and other operations on these geometric waveforms. The specification of specially adapted windows in Zak space to best make use of this relationship is a key component to the potential applications envisioned.

In this report we view the FZT as a stage in the Cooley-Tukey (CT) fast Fourier transform (FFT) algorithm. At this stage, the one-dimensional input data is arranged as a two (or higher)-dimensional data set and the algorithm proceeds by acting on this two-dimensional data set. The advantage of viewing this computation in this two-dimensional setting is that we can analyze the computation geometrically. We have used this approach to construct an orthogonal eigen vector basis of the N-point FT.

The CT FFT is an example of a divide-and-conquer algorithm. This important class of algorithms is standard in many DSP computations. Typically in this approach a one-dimensional data set is transformed into a multi-dimensional data set and the processing proceeds by operating on this multi-dimensional data set. For each of these algorithms we can exploit geometric methods.

The following notation will be used throughout this report. A vector $\mathbf{x} \in \mathbf{C}^N$ is written

$$\mathbf{x} = \begin{bmatrix} x_0 \\ x_1 \\ \vdots \\ x_{N-1} \end{bmatrix} = [x_n]_{0 \le n < N}$$

and

$$\mathbf{x}^K = [x_n]_{0 \le n < K}.$$

The inner product of two vectors $\mathbf{x}$ and $\mathbf{y}$ in $\mathbf{C}^N$ is

$$\langle \mathbf{x}, \mathbf{y} \rangle = \sum_{n=0}^{N-1} x_n y_n^*,$$

where $*$ denotes complex conjugation.

$\mathbf{e}_n^N$, $0 \le n < N$, is the vector in $\mathbf{C}^N$ having 1 in the n-th component and 0 in all other components. The set

$$\{\mathbf{e}_n^N : 0 \le n < N\}$$

is an orthonormal basis of $\mathbf{C}^N$.

$\mathbf{d}_n^N$, $0 \le n < N$, is the vector in $\mathbf{C}^N$ defined by

$$\mathbf{d}_n^N = \begin{bmatrix} 1 \\ w^n \\ \vdots \\ w^{n(N-1)} \end{bmatrix} = [w^{nm}]_{0 \le m < N}, \quad w = e^{2\pi i \frac{1}{N}}.$$

The set

$$\{\mathbf{d}_n^N : 0 \le n < N\}$$

is an orthogonal basis of $\mathbf{C}^N$ with

$$\langle \mathbf{d}_n^N, \mathbf{d}_n^N \rangle = N.$$

$F(N)$ is the N-point Fourier transform matrix

$$F(N) = [w^{mn}]_{0 \le m,\, n < N}.$$

We see that

$$F(N)\mathbf{e}_n^N = \mathbf{d}_n^N, \quad 0 \le n < N.$$

For $\mathbf{x} \in \mathbf{C}^N$, $D(\mathbf{x})$, is the $N \times N$ diagonal matrix

$$D(\mathbf{x}) = \begin{bmatrix} x_0 & & 0 & & \\ & x_1 & & & \\ & & \cdot & & \\ & & & \cdot & \\ & & & & \cdot \\ & & 0 & & x_{N-1} \end{bmatrix}.$$

D_N is the $N \times N$ diagonal matrix

$$D_N = D\left(\mathbf{d}_1^N\right)$$

and $D_N(K)$ is the $K \times K$ diagonal matrix

$$D_N(K) = D\left(\left(\mathbf{d}_1^N\right)^K\right).$$

S_N is the $N \times N$ cyclic shift matrix defined by

$$S_N\mathbf{y} = \begin{bmatrix} y_{N-1} \\ y_0 \\ \vdots \\ y_{N-2} \end{bmatrix}, \quad \mathbf{y} \in \mathbf{C}^N.$$

D_N and S_N are related by

$$F(N)S_N F(N)^{-1} = D_N,$$

and by

$$D_N^r S_N^{r'} = e^{2\pi i \frac{rr'}{N}} S_N^{r'} D_N^r, \quad r,\ r' \in \mathbf{Z}.$$

The N-point time-reversal matrix R_N is defined by

$$R_N \mathbf{y} = \begin{bmatrix} y_0 \\ y_{N-1} \\ \vdots \\ y_1 \end{bmatrix}, \quad \mathbf{y} \in \mathbf{C}^N.$$

Since

$$F(N)^{-1} = \frac{1}{N} F(N)^*,$$

we have

$$F(N) = NF(N)^{-1} R_N.$$

2 Chirps

A *chirp pulse* is any signal of the form

$$x_a(t) = \begin{cases} e^{\pi i \gamma t^2} e^{2\pi i \beta t}, & 0 \le t < T, \\ 0, \quad \text{otherwise}, \end{cases} \qquad t \in \mathbf{R}.$$

T is the time duration, γ is the chirp rate and β is the carrier frequency of the chirp x_a. Assume throughout that

$$N = \gamma T^2$$

is a positive integer. The methods developed in this report apply to a single transmission of x_a. In future work we will extend these methods to multiple chirp transmissions as in a SAR system and to chirp trains perhaps with varying time-duration, chirp rates and carrier frequencies.

γT is usually taken as an approximation to the bandwidth of x_a.

Sampling x_a at the points

$$\frac{n}{N} T = \frac{n}{\gamma T}, \quad n \in \mathbf{Z},$$

we form the *critically sampled chirp*

$$x_s(n) = x_a\left(\frac{n}{N} T\right) = \begin{cases} e^{\pi i \frac{n^2}{N}} e^{2\pi i f \frac{n}{N}}, & 0 \le n < N, \\ 0, \quad \text{otherwise}, \end{cases} \qquad n \in \mathbf{Z},$$

where $f = \beta T$.

If the chirp x_a is transmitted at a point and travels a distance r to a reflector P, then the echo at the point is

$$\alpha x_a(t - t_r), \quad t_r = \frac{2r}{c}.$$

α is a complex constant called the *scattering coefficient* of the reflector P. It includes amplitude attenuation as well as reflector reflectivity. The echo from multiple reflectors P_j, $0 \le j < J$, is

$$e_a(t) = \sum_{j=0}^{J-1} \alpha(j) x_a(t - t_{r_j}), \quad t \in \mathbf{R}.$$

In an *ideal* model a multiple point target return satisfies

$$t_{r_j} = n_j \frac{T}{N}, \quad n_j \in \mathbf{Z},\ 0 \le j < J,$$

and the *critically sampled echo* has the form

$$e_s(m) = e_a\left(m\frac{T}{N}\right) = \sum_{j=0}^{J-1} \alpha(j) x_s\left(m - n_j\right), \quad m \in \mathbf{Z}.$$

The ideal model will be assumed throughout this report except in 15.4. However the results in this report can be easily extended to the following perturbation of the ideal model. Suppose R is the distance between an antenna and a point taken as the origin in an xyz-coordinate system such that

$$\frac{2R}{c} = n_0 \frac{T}{N}, \quad n_0 \ge 0, \text{ an integer.}$$

If r is the distance between the antenna and a point in the ellipsoid

$$x^2 + y^2 + \frac{z^2}{\frac{T}{N}\frac{1}{4R}} \le R\frac{T}{N},$$

then

$$t_r = \frac{2r}{c} = n_0 \frac{T}{N} + \epsilon,$$

where

$$|\epsilon| \le \frac{T}{N}\frac{1}{c}.$$

For

$$0 \le \frac{n}{N}T - t_r < T, \quad n \in \mathbf{Z}$$

we have

$$x_a(\frac{n}{N}T - t_r) = e^{\pi i \gamma \epsilon^2} e^{-2\pi i \gamma \left(\frac{n-n_0}{N}\right) T\epsilon} e^{\pi i \gamma \left(\frac{n-n_0}{N}T\right)^2} e^{2\pi i \beta \left(\frac{n-n_0}{N}\right) T} e^{-2\pi i \beta \epsilon}.$$

Since

$$\gamma\left(\frac{n-n_0}{N}\right) T|\epsilon| \le \frac{n-n_0}{N}\frac{1}{c},$$

we can up to a high degree of accuracy set

$$e^{\pi i \gamma \epsilon^2} e^{-2\pi i \gamma \left(\frac{n-n_0}{N}\right) T\epsilon} = 1$$

and set

$$x_a\left(\frac{n}{N}T - t_r\right) = e^{\pi i\frac{(n-n_0)^2}{N}} e^{2\pi i f\frac{n-n_0}{N}} e^{-2\pi i\beta\epsilon}, \quad f = \beta T.$$

Suppose $0 < \epsilon$. Assuming the periodicity condition

$$e^{\pi i N} e^{2\pi i f} = 1,$$

since $0 < \epsilon < \frac{T}{N}$, we have

$$x_a\left(n\frac{T}{N} - t_r\right) = e^{-2\pi i\beta\epsilon} y(n),$$

where

$$y(n_0 + m) = \begin{cases} x_s(m), & 0 \le m < N-1, \\ x_s(0), & m = N, \\ 0, & \text{otherwise} \end{cases} \qquad m \in \mathbf{Z}.$$

The perturbation from the ideal model introduces a shift which will be more fully described in 15.4 and a carrier frequency dependent phase factor.

The preceding discussion can be modified depending on the degree of accuracy required. Suppose $\Delta > 0$ is such that the approximation

$$e^{-2\pi i\frac{n}{N}\frac{\Delta}{c}} = 1, \quad 0 \le n < N,$$

is acceptable. If r is the distance between the antenna and a point in the ellipsoid

$$x^2 + y^2 + \frac{z^2}{\frac{T}{N}\frac{\Delta}{4R}} \le \frac{T}{N} R\Delta,$$

then

$$t_r = \frac{2r}{c} = \frac{2R}{c} + \epsilon,$$

where

$$|\epsilon| \le \frac{T}{N}\frac{\Delta}{c}.$$

Arguing as before we have the approximation

$$x_a\left(n\frac{T}{N} - t_r\right) = e^{-2\pi i\beta\epsilon} y(n), \quad n \in \mathbf{Z},$$

where

$$y(n_0 + m) = \begin{cases} x_s(m), & 1 \le m < N, \\ x_s(0), & m = N, \\ 0, & \text{otherwise,} \end{cases} \qquad m \in \mathbf{Z}.$$

Allowing for zero scattering coefficients we can write e_s as

$$e_s(m) = \sum_{n=0}^{(R-1)N-1} \alpha(n) x_s(m-n), \quad m \in \mathbf{Z},$$

for a sufficiently large integer R. A coefficient of this expansion may be the sum of the scattering coefficients of reflectors equidistant to the transmitter/receiver. We call this expansion for e_s the *discrete echo model* for the critically sampled chirp x_s. The critically sampled echo e_s is the input for processing. The problem is to compute the scattering coefficients $\alpha(n)$, $0 \leq n < (R-1)N$, from the input e_s. In Section 7 we begin developing methods for solving the problem in the finite Zak transform framework.

In Section 7 we begin with an $\mathbf{x} \in \mathbf{C}^N$ and define $\mathbf{x}^{RN} \in \mathbf{C}^{RN}$ by

$$\mathbf{x}^{RN} = \begin{bmatrix} \mathbf{x} \\ \mathbf{0}^N \\ \vdots \\ \mathbf{0}^N \end{bmatrix}, \quad R-1 \text{ copies of } \mathbf{0}^N.$$

An *echo* of $\mathbf{x}^{RN}$ is any linear combination

$$\mathbf{e} = \sum_{n=0}^{(R-1)N-1} \alpha(n) S_{RN}^n \mathbf{x}^{RN},$$

where S_{RN} is the $RN \times RN$ shift matrix. The summation is taken so that there is no aliasing due to periodicity modulo RN and the cyclic shifts are linear shifts. The theory developed in this report equally applies to multiple copies of $\mathbf{x}^{RN}$.

The spatial resolution of x_a is usually taken as $\frac{cT}{2}$. However, as we will see, by orthogonality we can distinguish two targets whose distances from the an antenna differ by

$$c\frac{T}{N} = \frac{c}{\gamma T}$$

and so we will call $\frac{c}{\gamma T}$ the *resolution* of the critically sampled chirp x_s. To achieve finer resolution we can increase γT. In future work we will approach the problem of finer resolution by over sampling. This method is based on sampling x_a at the points

$$\frac{m}{KN}T, \quad m \in \mathbf{Z},$$

where K is a fixed positive integer. The resulting *oversampled chirp*

$$x_{ov}(m) = x_a\left(\frac{m}{KN}T\right) = \begin{cases} e^{\pi i \frac{m^2}{K^2 N}} e^{2\pi i f \frac{m}{KN}}, & 0 \leq m < KN, \\ 0, \quad \text{otherwise}, \end{cases}$$

can be decomposed into K sequences $x_{ov}^{(k)}$, $0 \leq k < K$,

$$x_{ov}^{(k)}(n) = x_{ov}(k+nK) = x_{ov}(k) x_s(n) e^{2\pi i \frac{kn}{KN}}, \quad n \in \mathbf{Z},$$

where x_s is the critically sampled chirp.

3 Discrete Chirps

In the first part of this report we develop the *algebra* of discrete chirps in the framework of the finite Zak transform (FZT). The results of this part will be the basis for studying critically sampled echoes beginning in Section 8.

A *discrete chirp* is any sequence of the form

$$x(n) = e^{\pi i \frac{n^2}{N}} e^{2\pi i f \frac{n}{N}}, \quad n \in \mathbf{Z},$$

which is periodic modulo N,

$$x(n+N) = x(n), \quad n \in \mathbf{Z}.$$

The periodic modulo N condition is equivalent to

$$N + 2f \in 2\mathbf{Z}.$$

Throughout this report we identify the linear space of periodic modulo N sequences with $\mathbf{C}^N$ by setting

$$\mathbf{y} = \begin{bmatrix} y(0) \\ y(1) \\ \vdots \\ y(N-1) \end{bmatrix} = [y(n)]_{0 \le n < N}.$$

S_N is the N-point cyclic shift matrix. A *cyclic echo* of $\mathbf{y} \in \mathbf{C}^N$ is any linear combination

$$\mathbf{e} = \sum_{r=0}^{N-1} \alpha(r) S_N^r \mathbf{y}.$$

If $\mathbf{x}$ is a discrete chirp, then the cyclic echo expansion

$$\mathbf{e} = \sum_{r=0}^{N-1} \alpha(r) S_N^r \mathbf{x}$$

is an orthogonal expansion and its coefficients can be computed from N inner products, a special case of match filtering.

If $\mathbf{x}$ is a discrete chirp, then the multiplication operator $M_{\mathbf{x}^*}$ is called $\mathbf{x}$-dechirping. The $\mathbf{x}$-dechirping of a cyclic echo $\mathbf{e}$ of $\mathbf{x}$ is

$$M_{\mathbf{x}^*}\mathbf{e}(n) = \sum_{r=0}^{N-1} \alpha(r) x(-r) e^{-2\pi i \frac{nr}{N}}, \quad n \in \mathbf{Z}.$$

Dechirping provides a second way to compute the coefficients of a cyclic echo $\mathbf{e}$ of a discrete chirp $\mathbf{x}$. First $\mathbf{x}$-dechirp the cyclic echo, compute its N-point FT and diagonal matrix multiply the result by the inverse of

$$ND\left([x(-r)]_{0 \le r < N}\right).$$

4 Finite Zak Transform (FZT)

In this section we introduce the finite Zak transform (FZT). For each positive divisor L of N we define a linear isomorphism

$$Z_L : \mathbf{C}^N \longrightarrow \mathbf{C}^L \times \mathbf{C}^K, \quad N = LK,$$

of $\mathbf{C}^N$ onto $\mathbf{C}^L \times \mathbf{C}^K$. If $\mathbf{y} \in \mathbf{C}^N$, then $Z_L\mathbf{y}$ is a two-dimensional $L \times K$ time-frequency image of $\mathbf{y}$.

For a positive divisor L of N and $\mathbf{y} \in \mathbf{C}^N$ construct the vectors $\mathbf{z}_k$, $0 \leq k < K$, in $\mathbf{C}^L$,

$$\mathbf{z}_k = \begin{bmatrix} y_k \\ y_k + K \\ \vdots \\ y_{k+(L-1)K} \end{bmatrix} = [y_{k+lK}]_{0 \leq l < L}.$$

$\mathbf{z}_k$ is the subvector in $\mathbf{C}^L$ formed by the components of $\mathbf{y}$ over the index set

$$\{k + lK : 0 \leq l < L\}.$$

The sequence

$$\mathbf{z}_0, \ \mathbf{z}_1, \ \ldots, \ \mathbf{z}_{K-1}$$

describes the evolution of these subvectors. If $L = 1$, we have the standard ordering of the components of $\mathbf{y}$. For $L = 2$, we have a description of the evolution from the even components to the odd components of $\mathbf{y}$.

Identify $\mathbf{C}^L \times \mathbf{C}^K$ with the space of $L \times K$ complex matrices. Define the mapping $M_L : \mathbf{C}^N \longrightarrow \mathbf{C}^L \times \mathbf{C}^K$ by

$$M_L\mathbf{y} = [\mathbf{z}_0 \ \mathbf{z}_1 \ \cdots \ \mathbf{z}_{K-1}], \quad \mathbf{y} \in \mathbf{C}^N,$$

and the mapping $Z_L : \mathbf{C}^N \longrightarrow \mathbf{C}^L \times \mathbf{C}^K$ by

$$Z_L\mathbf{y} = F(L)M_L\mathbf{y}, \quad \mathbf{y} \in \mathbf{C}^N.$$

$Z_L\mathbf{y}$ provides a two-dimensional $L \times K$ image of the evolution of the FT of the sequence of subvectors.

$Z_L\mathbf{y}$, $\mathbf{y} \in \mathbf{C}^N$, is called the $L \times K$ FZT of $\mathbf{y}$ or more suggestively, the $L \times K$ Zak space representation of $\mathbf{y}$. Different factorizations of N lead to different Zak space representations each depicting different time-frequency aspects of $\mathbf{y}$ in the sense discussed. For example $Z_1\mathbf{y}$ is the transpose of $\mathbf{y}$ while $Z_N\mathbf{y}$ is the N-point FT of $\mathbf{y}$. Throughout this report the theory is developed for a single factorization of N. A future effort will be directed toward combining two or more Zak space representations for the purpose of echo analysis and noise reduction.

Z_L is a linear isomorphism of $\mathbf{C}^N$ onto $\mathbf{C}^L \times \mathbf{C}^K$ with inverse

$$Z_L^{-1} = M(L)^{-1}F(L)^{-1}.$$

Up to scale factor Z_L is an isometry.

$$|Z_L\mathbf{y}|^2 = L|\mathbf{y}|^2, \quad \mathbf{y} \in \mathbf{C}^N.$$

An orthogonal basis in $\mathbf{C}^N$ is mapped onto an orthogonal basis in $\mathbf{C}^L \times \mathbf{C}^K$.

In this section we derive general formulas relating the FZT of a signal with that of its cyclic shifts. Suppose $\mathbf{x}$ is a vector in $\mathbf{C}^N$ and set

$$Z_L\mathbf{x} = [X_0\ X_1\ \cdots\ X_{K-1}], \quad X_k \in \mathbf{C}^L.$$

The FZT of the cyclic shift of a signal is not simply the cyclic shift of the columns of the FZT of the signal. The cyclic shift has its 0-th column multiplied by D_L and more generally

$$Z_L\left(S_N^{nK}\mathbf{x}\right) = D_L^n Z_L\mathbf{x}, \quad 0 \le n < L.$$

In this case the columns of $Z_L\mathbf{x}$ are multiplied by D_L^n.

For $\mathbf{x}$ and $\mathbf{y}$ in $\mathbf{C}^N$, the N-point *cyclic convolution* is defined by

$$\mathbf{u} = \mathbf{x} * \mathbf{y} = \sum_{r=0}^{N-1} x_r S_N^r \mathbf{y}.$$

5 FZT and CT Factorization

There are several ways to motivate the definition of the FZT. We choose the approach to the FZT most directly related to computation. The FZT can be viewed as an implementation of two stages of the Cooley-Tukey (CT) FFT algorithm. We approach the CT FFT algorithm through factorizations of the N-point FT matrix $F(N)$.

We continue to use the notation in Section 4. The $N \times N$ stride permutation matrix $P(N,K)$ is defined by

$$P(N,K)\mathbf{y} = [\mathbf{z}_k]_{0 \le k < K}, \quad \mathbf{y} \in \mathbf{C}^N.$$

$I_K \otimes F(L)$ is the $N \times N$ block diagonal matrix

$$I_K \otimes F(L) = \begin{bmatrix} F(L) & & 0 \\ & \ddots & \\ 0 & & F(L) \end{bmatrix}.$$

Set z_L equal to the $N \times N$ matrix

$$z_L = (I_K \otimes F(L))\, P(N,K).$$

In [7], we show

$$F(N) = K z_K^{-1} \left((I_L \otimes R_K)\, P(N,L) T_N(L)\right) z_L,$$

where R_K is K-point time-reversal and $T_N(L)$ is a diagonal matrix whose diagonal entries are N-th roots of unity.

It is convenient and standard to view the N-point CT FFT as given by this CT factorization as a multi-stage process in which a vector $\mathbf{y} \in \mathbf{C}^N$ is first mapped onto a two-dimensional array, operations are performed on the two-dimensional array and then the two-dimensional array is mapped back to the vector $F(N)\mathbf{y}$.

CT FFT computation of $F(N)\mathbf{y}$, $\mathbf{y} \in \mathbf{C}^N$

- Form the $L \times K$ array $M_L\mathbf{y}$.
- Compute the L-point FT of every column of $M_L\mathbf{y}$.

$$Z_L\mathbf{y} = F(L)M_L\mathbf{y}.$$

These two stages correspond to the matrix product $z_L\mathbf{y}$.

- Multiply the coefficients of the $L \times K$ array $Z_L\mathbf{y}$ by N-th roots of unity as determined by $T_N(L)$.
- Transpose the resulting array to form a $K \times L$ array.
- Compute the K-point time-reversal of each column of the transposed $K \times L$ array.

The preceding two stages correspond to operating by the permutation matrix $R_N P(N, L)$.

- Form $F(N)\mathbf{y}$ by operating on the $K \times L$ array by KZ_K^{-1}.

The final stage correspond to matrix multiplication by Kz_K^{-1}.

6 FZT of Dechirped Echo

Throughout set $w = e^{2\pi i \frac{1}{N}}$ and $v = e^{2\pi i \frac{1}{L}}$.

In this section we compute the FZT of a dechirped cyclic echo of a discrete chirp $\mathbf{x}$

$$\mathbf{e} = \sum_{r=0}^{N-1} \alpha(r) S_N^r \mathbf{x}$$

and compare the result with the FT of $\mathbf{e}$.

Define the $L \times K$ matrix $F_K^L(r)$, $r \in \mathbf{Z}$, by

$$F_K^L(r) = \left[\mathbf{e}_r^L \cdots \mathbf{e}_r^L\right].$$

We can view $F_K^L(r)$ as a horizontal line in $L \times K$ Zak space at position $r \bmod L$.

Set $\mathbf{y} = M_{\mathbf{x}^*} S_N^r \mathbf{x}$, $0 \le r < N$. To compute the k-th column of $Z_L \mathbf{y}$ form the k-th column of $M_L \mathbf{y}$

$$[y_{k+lK}]_{0 \le l < L} = x(-r) w^{-rk} \left[v^{-rk} \right]_{0 \le l < L} = x(-r) w^{-rk} \mathbf{d}_{-r}^L,$$

and then take its L-point FT

$$Lx(-r) w^{-rk} \mathbf{e}_r^L.$$

Figure 1 displays the Zak transform of dechirped discrete chirp and its cyclic shifts. The two-dimensional intensity data are displayed as log-scaled images. The discrete chirp parameters are $\gamma = .25$, $T = 80$, $f = 40$. $N = \gamma T^2 = 1600$. The FZT parameters are $L = 50$ and $K = 32$.

Figure 1: Zak transform of dechirped discrete chirp

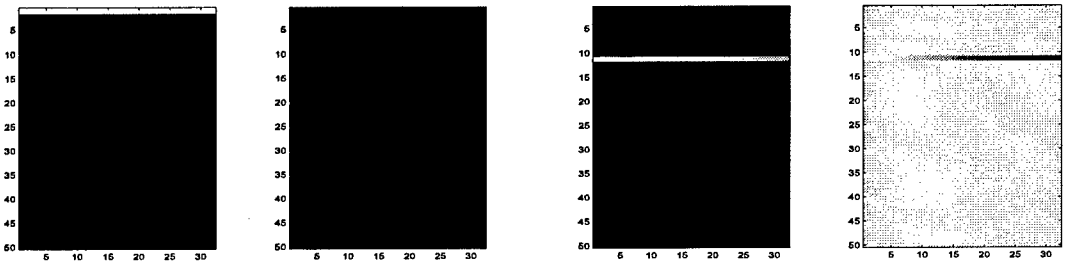

real part imaginary part real part imaginary part

cyclic shift by 10

We have that

$$\{S_N^r \mathbf{x} : 0 \le r < N\}$$

is an orthonormal basis of $\mathbf{C}^N$ and the set

$$\{Z_L (M_{\mathbf{x}^*} S_N^r \mathbf{x}) : 0 \le r < N\}$$

is an orthogonal basis of $\mathbf{C}^L \times \mathbf{C}^K$.

Since the support of the $L \times K$ Zak space representation of $M_{\mathbf{x}^*} S_N^r \mathbf{x}$ is the horizontal line at position $r \ mod \ L$, if

$$r \equiv r' \ mod \ L, \quad 0 \le r, \ r' < N,$$

we cannot distinguish the vectors

$$M_{\mathbf{x}^*} S_N^r \mathbf{x} \text{ and } M_{\mathbf{x}^*} S_N^{r'} \mathbf{x}$$

by the supports of their $L \times K$ Zak space representations. However if

$$r \not\equiv r' \ mod \ L, \quad 0 \le r, \ r' < N,$$

then the supports of the $L \times K$ Zak space representations of these vectors are disjoint. In particular the supports of

$$\{Z_L\left(M_{\mathbf{x}^*} S_N^r \mathbf{x}\right): \quad 0 \le r < L\}$$

are pairwise disjoint.

Generally the support of the $L \times K$ Zak space representation of $M_{\mathbf{x}^*} S_N^r \mathbf{x}$ determines $r \ mod \ L$ but not r itself. To compute r we must look at the values of $Z_L\left(M_{\mathbf{x}^*} S_N^r \mathbf{x}\right)$ on the horizontal line at position $r \ mod \ L$ with values given by the vector $\mathbf{v} \in \mathbf{C}^K$

$$\mathbf{v} = Lx(-r)\left[w^{-rk}\right]_{0 \le k < K}. \tag{1}$$

Write

$$r = a + bL, \quad 0 \le a < L, \ 0 \le b < K.$$

a is known and b is to be determined. Then

$$\mathbf{v} = Lx(-(a+bL))D_N^{-a}(K)\left[u^{-bk}\right]_{0 \le k < K}, \quad u = e^{2\pi i \frac{1}{K}}.$$

To determine b we compute

$$F(K)D_N^a(K)\mathbf{v} = c\mathbf{e}_b^K,$$

where c is the complex constant

$$c = Nx(-(a+bL)).$$

b is determined as the index of *nonzero* component of the computation.

Figures 2 and 3 displays the Zak transform of dechirped, cyclically shifted discrete chirps. The shift amounts are of the form $a + bL$, $a = 11$, and all congruent modulo $L = 50$. The second row of the figure are plots of the values on the horizontal line through a. The third row of the figure are plots of the vector $F(K)D_N(K)^a = c\mathbf{e}_b^K$. Note that the position of nonzero value corresponds to b.

For a cyclic echo $\mathbf{e}$ of a discrete chirp $\mathbf{x}$

$$\mathbf{e} = \sum_{r=0}^{N-1} \alpha(r) S_N^r \mathbf{x},$$

we have

$$Z_L\left(M_{\mathbf{x}^*}\mathbf{e}\right) = L \sum_{r=0}^{N-1} \alpha(r) x(-r) F_K^L(r) D_N^{-r}(K).$$

Since the set

$$\{x(-r)F_K^L(r)D_N^{-r}(K) : 0 \le r < N\}$$

is an orthogonal basis of $\mathbf{C}^L \times \mathbf{C}^K$, we can compute the coefficients $\alpha(r)$, $0 \le r < N$, by inner products.

There are two important special cases for applications. Suppose

$$\mathbf{e} = \sum_{r=0}^{L-1} \alpha(r) S_N^r \mathbf{x}.$$

Figure 2: Zak transform of dechirped discrete chirp

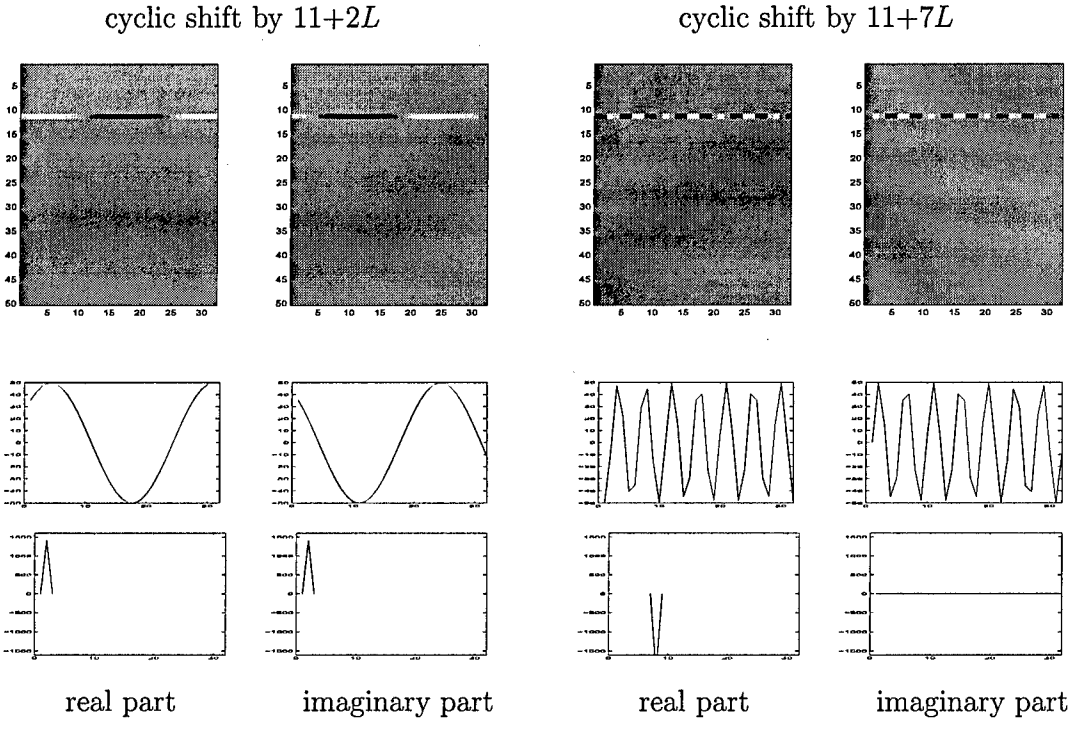

We say that $\mathbf{e}$ is a cyclic echo from *closely spaced targets.* The values of $Z_L(M_{\mathbf{x}^*}\mathbf{e})$ on the horizontal line at position $0 \le r < L$ are given by the vector $\mathbf{v}_r \in \mathbf{C}^K$

$$\mathbf{v}_r = \alpha(r)x(-r)\left[w^{-rk}\right]_{0\le k<K},$$

where we have divided out L. For simplicity in the discussion assume the coefficients of $\mathbf{e}$ are positive real numbers or zero. Then

$$|\mathbf{v}_r| = \begin{bmatrix} \alpha(r) \\ \vdots \\ \alpha(r) \end{bmatrix}.$$

In the presence of noise we may have errors attached to the coefficients of $|\mathbf{v}_r|$. We can estimate $\alpha(r)$ by best estimation techniques on the K components of the noisy $|\mathbf{v}_r|$. Figures 4 – 6 illustrates results of this denoising method. Figure 4 displays the noise-free cyclic echo which is the sum of 5 cyclically shifted chirps with non-negative coefficients. The shifts are 9, 17, 26, 30, 32 and the respective coefficients are 0.5992, 3.0385, 0.9145, 1.8699, 1.7293. Figure 5 displays the noisy echo obtained by adding noise to the cyclic echo in Figure 4.

The Zak transform of the dechirped noisy echo is used as input to image processing algorithm for detecting and locating the horizontal lines. Location is exact in this case.

Figure 4: Noise-free cyclic echo

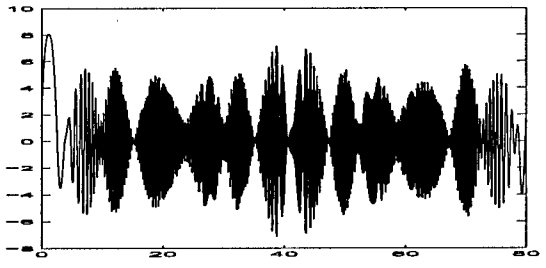

real part

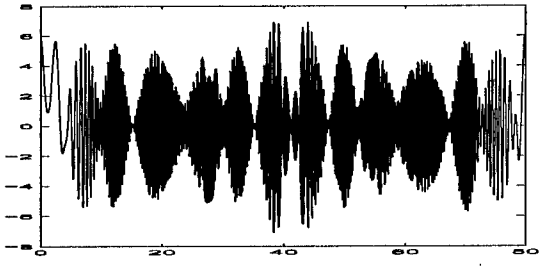

imaginary part

Figure 5: Noisy echo

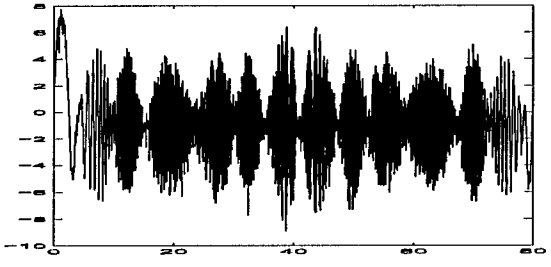

real part

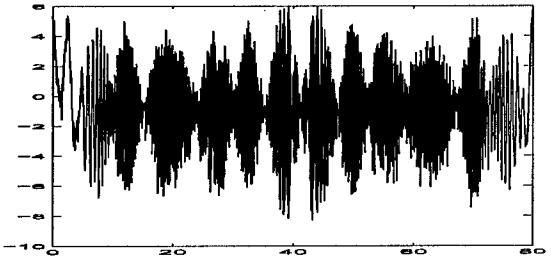

imaginary part

illustrate estimation of arbitrary scattering coefficients. The discrete chirp parameters are $\gamma = .25$, $f0 = 40$, $N = 1600$. Figure 12 displays the noise free echo which is the sum of 4 cyclically shifted discrete chirps. The Zak transform parameters are $L = 40$, $K = 40$.

The estimated shifts are accurate at 10, 16, 23, 29. In Figure 16 plots of the absolute values of the ratio of the detected horizontal lines and the corresponding vectors given in (1).

Table 3 compares the test values with estimated values of the scattering coefficients.

The FT approach essentially sums these errors to a single noisy component by a K-point FT computation.

The same argument holds for a cyclic echo of a discrete chirp $\mathbf{x}$ of the form

$$\mathbf{e} = \sum_{r=0}^{L-1} \alpha(r) S_N^{r+r_0} \mathbf{x}, \quad r_0 \text{ some integer.}$$

Observe that the Zak space representation of $\mathbf{e}$ does not directly determine the *first* target. r_0 must be known either from the application or computed by the above discussion. In future work we will study the use of the information gained from several size FZT computations to remove ambiguities of this kind.

Figure 6: dB plot of signal to noise ratio

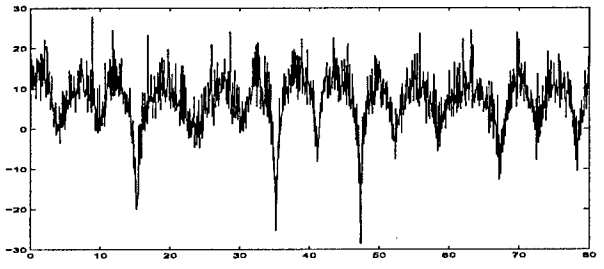

Figure 7: Zak transform of the dechirped noisy echo

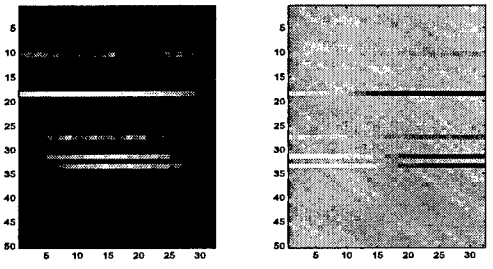

Assume that the target structure is *sparse* relative to the sampling in the sense that there are relatively few horizontal lines in the Zak space image of the dechirped echo as compared with L. Since we know that the FZT of a noise free dechirped echo must be supported on horizontal lines we can search Zak spaces for the existence and positions of these lines, determine noise statistics under the knowledge that the Zak space representation of the dechirped cyclic echo must vanish off of the lines and use the noise statistics to correct for noise on the lines themselves. In the first line determination step if there are any variations in the line structures, we can correct these variations by best line approximation methods.

For sparse target structures the FZT approach restricts scattering coefficient computation to nonvanishing lines in Zak space while the FT approach requires computation for every horizontal line in Zak space.

7 FZT of Discrete Chirps

In this section we describe the FZT of discrete chirps. Dechirping is a powerful tool for the applications considered in Section 6 using either the FT or FZT. However one of the goals of this report is to show how the framework of FZT can be used to analyze echoes in a more general setting than that obtained in Section 6. For example the framework should allow for multiple chirp sets and chirp pulses, perhaps at varying chirp rates and should include tools

Figure 8: Noise-free cyclic echo

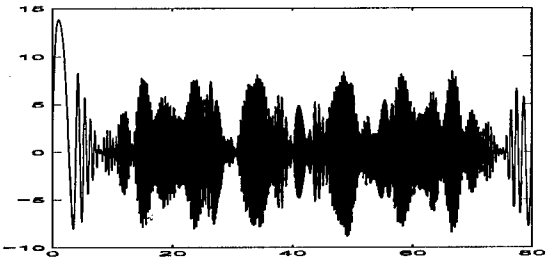

real part

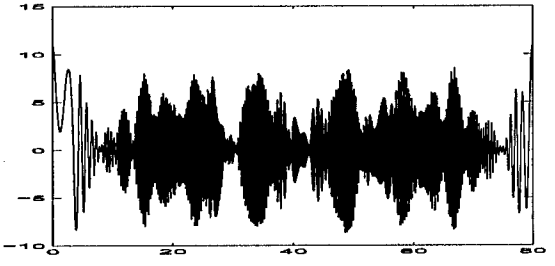

imaginary part

Figure 9: Noisy echo

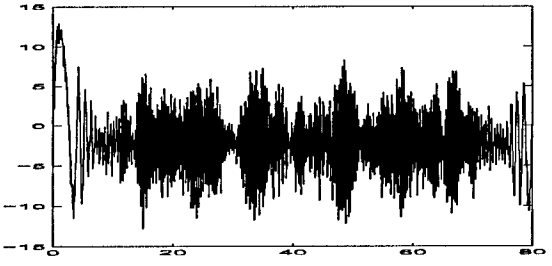

real part

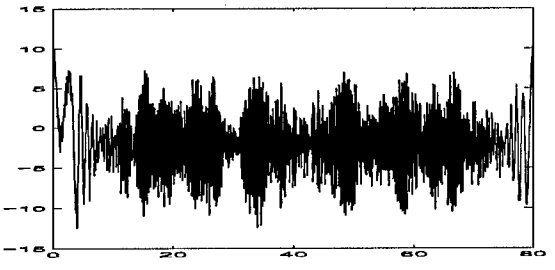

imaginary part

for realizing linear shifts as well as cyclic shifts. The results of this section provide the basis for these extensions which will be addressed in future work. At the same time these results will suggest the use of the Zak space framework in waveform design, another topic in future work.

Define the $L \times K$ matrix $E_K^L(0)$ by

$$E_K^L(0) = \left[\mathbf{e}_0^L \, \mathbf{e}_{-1}^L \, \cdots \, \mathbf{e}_{-(K-1)}^L\right].$$

As usual $\mathbf{e}_m^L$ is defined for $m \; mod \; L$. We can view $E_K^L(0)$ as the line of slope 1 through the origin.

Set

$$C_0 = F(L) Diag\left[x(lK)\right]_{0 \le l < L} F(L)^{-1}.$$

The support of

$$C_0^{-1} Z_L \mathbf{x} = L E_K^L(0) D\left(\mathbf{x}_K\right)$$

is $E_K^L(0)$, the line of slope 1 through the origin.

Define the $L \times K$ matrix $E_K^L(r)$ by

$$E_K^L(r) = \left[\mathbf{e}_r^L \, \mathbf{e}_{r-1}^L \, \cdots \, \mathbf{e}_{r-(K-1)}^L\right], \quad r \in \mathbf{Z}.$$

Figure 10: dB plot of signal to noise ratio

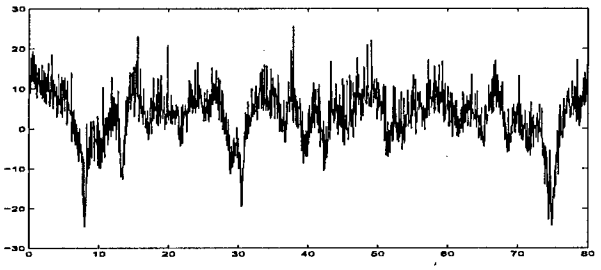

Figure 11: Zak transform of the dechirped noisy echo

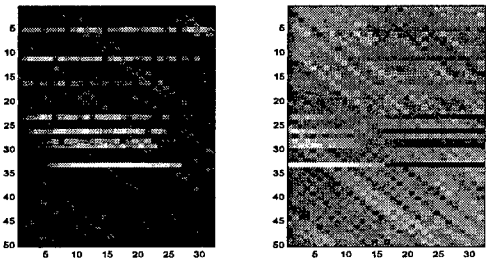

We can view $E_K^L(r)$ as the line of slope 1 through the point $(r, 0)$ in $L \times K$ Zak space. As with the horizontal lines $F_K^L(r)$ in Section 6, we have that

$$E_K^L(r) = E_K^L(r'), \quad r,\ r' \in \mathbf{Z},$$

if and only if

$$r \equiv r' \ mod\ L$$

and that

$$E_K^L(r) \text{ and } E_K^L(r'), \quad r,\ r' \in \mathbf{Z},$$

are disjoint whenever

$$r \not\equiv r' \ mod\ L.$$

In particular the lines of slope 1

$$\left\{E_K^L(r): \quad 0 \le r < L\right\},$$

are pairwise disjoint in $\mathbf{C}^L \times \mathbf{C}^K$.

As before, the set

$$Z_L\left(S_N^r \mathbf{x}\right), \quad 0 \le r < N,$$

is an orthogonal basis in $\mathbf{C}^L \times \mathbf{C}^K$. Since C_0 is a unitary matrix we have that the set

$$\{C_0^{-1} Z_L\left(S_N^r \mathbf{x}\right) : 0 \le r < N\}$$

Table 2: comparison of estimated scattering coefficients

test coefficients	1.0824	1.2694	0.6954	1.5013	2.1946	1.6165	1.8878	3.9520
average coefficients	1.0263	1.2099	0.7001	1.5277	2.1236	1.5740	1.8178	3.9048
median coefficients	1.0968	1.2717	0.6831	1.5904	2.1976	1.5031	1.8072	3.8628

Figure 12: Noise-free cyclic echo

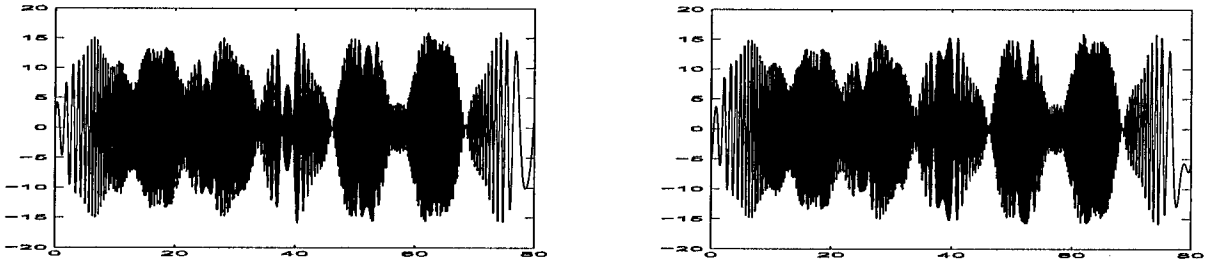

real part imaginary part

is also an orthogonal basis in $\mathbf{C}^L \times \mathbf{C}^K$.

Since the support of

$$C_0^{-1} Z_L\left(S_N^r \mathbf{x}\right) = L E_K^L(r) D\left(\mathbf{x}_K\right) D_N(K)^{-r}$$

is $E_K^L(r)$, the line of slope 1 through the point $(r, 0)$, the $L \times K$ Zak space representations

$$\left\{C_0^{-1} Z_L\left(S_N^r \mathbf{x}\right) : 0 \leq r < L\right\}$$

are pairwise disjoint.

The discussion in Section 6 on the use of the FZT operating on a dechirped cyclic echo can be directly carried over to the use of the FZT operating on a cyclic echo. The horizontal lines $F_K^L(r)$ are replaced by the lines $E_K^L(r)$ of slope 1.

The following condition is involved in theory and numerical experiments for notational simplicity. It removes the necessity of multiplying by C_0^{-1} to get a simple geometric interpretation of results.

We say that a discrete chirp $\mathbf{x}$ satisfies the $L \times K$ *Zak space condition* if

$$x(lK) = 1, \quad 0 \leq l < L.$$

The $L \times K$ Zak space condition is equivalent to the condition

$$l^2 M + 2f\frac{l}{L} \in 2\mathbf{Z}, \quad 0 \leq l < L,\ M = \frac{K}{L}.$$

The FT and the FZT of a dechirped cyclic shift of a discrete chirp $\mathbf{x}$ result in sparse outputs, a single nonzero component for the FT computation and a single horizontal line of

Figure 13: Noisy echo

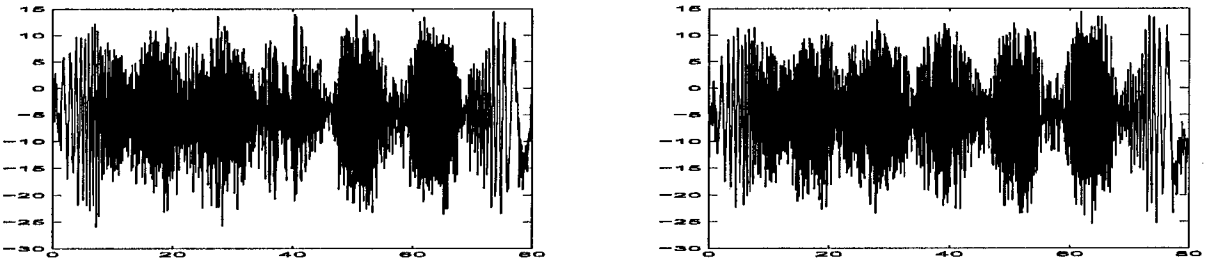

real part imaginary part

Figure 14: dB plot of signal to noise ratio

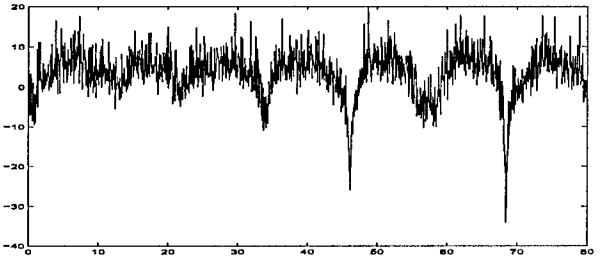

values for the FZT computation. We have just seen that the FZT of $\mathbf{x}$ is also sparse having support a single line of slope 1. The analogy collapses when computing the FT of $\mathbf{x}$.

Set

$$\mathbf{v} = F(N)\mathbf{x}.$$

A direct computation shows that

$$v_a = \sum_{n=0}^{N-1} w^{\frac{n^2}{2}} w^{(a+f)n}, \quad 0 \le a < N.$$

Suppose for example $N = 4$ and f is even. Then

$$\begin{aligned} v_0 &= 2i^{\frac{1}{2}} i^f, \\ v_1 &= 2, \\ v_2 &= -2i^{\frac{1}{2}} i^f, \\ v_3 &= 2. \end{aligned}$$

Figure 15: Zak transform of the dechirped noisy echo

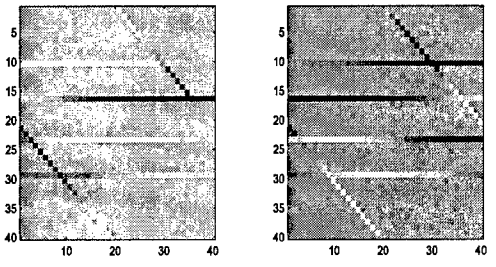

Figure 16: Magnitudes of the values on the detected lines/vectors given by (1)

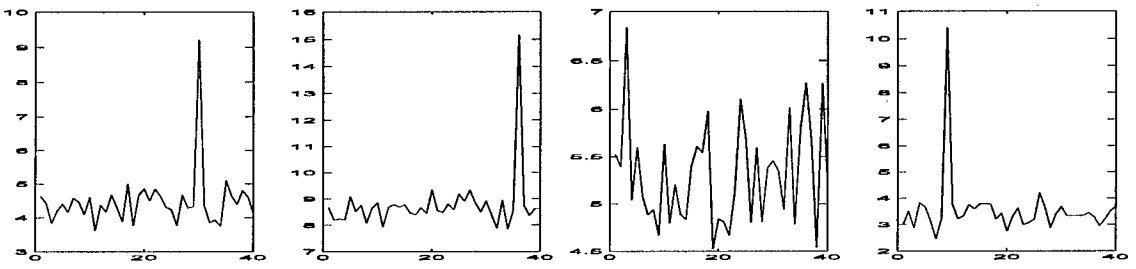

shift by 10 shift by 16 shift by 23 shift by 29

8 Zero-padding

In preceding sections, we developed the general theory of the FZT for vectors in $\mathbf{C}^N$ or equivalently for periodic modulo N sequences and applied the theory to discrete chirps and their cyclic shifts. The general theory will be extended to zero-padded vectors and applied to zero-padded discrete chirps and their linear shifts.

Suppose $\mathbf{x} \in \mathbf{C}^N$ and R is a positive integer. Define the zero-padding $\mathbf{x}^{RN}$ of $\mathbf{x}$ to $\mathbf{C}^{RN}$ by

$$\mathbf{x}^{RN} = \mathbf{e}_0^R \otimes \mathbf{x} = \begin{bmatrix} \mathbf{x} \\ \mathbf{0}^N \\ \vdots \\ \mathbf{0}^N \end{bmatrix}, \quad R-1 \text{ copies of } \mathbf{0}^N \text{ adjoined to } \mathbf{x}.$$

As discussed in Section 2, the cyclic shifts

$$S_{RN}^m \mathbf{x}^{RN}, \quad 0 \le m < (R-1)N,$$

are linear shifts.

We begin by describing the general theory of the FZT for zero-padded vectors. By making use of the special form of zero-padded vectors and the finer details of the RN-point CT FFT

Table 3: comparison of estimated scattering coefficients

test coefficients	1.5740+3.9952i	7.2175+4.7044i	-1.7549-4.9605i	3.1162+1.0602i
average coefficients	1.7173+4.0692i	7.3979+4.6806i	-1.5806-4.9725i	3.3206+1.1680i
median coefficients	4.3647+4.0759i	10.3068+4.7747i	0.9659-5.0327i	6.3260+1.4081i

algorithm, we show that the $RL \times K$ FZT of $\mathbf{x}^N$ consists of the $L \times K$ FZT of $\mathbf{x}$ over a region of $RL \times K$ Zak space and filtered versions of this FZT over other regions.

The cyclic shifts of $\mathbf{x}^{RN}$ are more difficult to handle in the $RL \times K$ FZT framework. The reason for this is that the Fourier transform does not commute with the shift operations. The general theory of linear shifts is studied in Section 10.

To compute the $RL \times K$ Zak space representation of $\mathbf{x}^{RN}$ we will first derive a formula for computing the RL-point FT of a zero-padded vector $\mathbf{u}^{RL}$, $\mathbf{u} \in \mathbf{C}^L$. The main tool needed is the CT FFT factorization for the RL-point Fourier transform. Recall the following tensor product notation.

$P(RL, L)$ is the $RL \times RL$ stride by L permutation matrix defined as follows. Suppose $\mathbf{v} \in \mathbf{C}^{RL}$. Form the vector $\mathbf{w}_0 \in \mathbf{C}^R$ by striding through $\mathbf{v}$ with stride L.

$$\mathbf{w}_0 = \begin{bmatrix} v_0 \\ v_L \\ \vdots \\ v_{(R-1)L} \end{bmatrix}.$$

Off-setting by 1, form the vector $\mathbf{w}_1$

$$\mathbf{w}_1 = \begin{bmatrix} v_1 \\ v_{L+1} \\ \vdots \\ v_{(R-1)L+1} \end{bmatrix}.$$

Continuing in this way, form the L vectors in $\mathbf{C}^R$

$$\mathbf{w}_0, \mathbf{w}_1, \ldots, \mathbf{w}_{L-1}.$$

Define

$$P(RL, L)\mathbf{v} = \begin{bmatrix} \mathbf{w}_0 \\ \mathbf{w}_1 \\ \vdots \\ \mathbf{w}_{L-1} \end{bmatrix}.$$

Define the $L \times L$ diagonal matrix $D_{RL}(L)$ by

$$D_{RL}(L) = D\left(\left[\tau^l\right]_{0 \le l < L}\right), \quad \tau = e^{2\pi i \frac{1}{RL}}$$

and the $RL \times RL$ diagonal matrix T_{RL} by

$$T_{RL}(L) = \bigoplus_{r=0}^{R-1} D_{RL}^{r}(L).$$

Set

$$C_{RL}(L) = F(L) D_{RL}(L) F(L)^{-1}$$

and

$$\mathbf{C}_{RL}(L) = \begin{bmatrix} I_L \\ C_{RL}(L) \\ \vdots \\ C_{RL}^{R-1}(L) \end{bmatrix}.$$

We will use the following CT factorization for $F(RL)$.

$$F(RL) = P(RL, L) \left(I_R \otimes F(L)\right) T_{RL}(L) \left(F(R) \otimes I_L\right).$$

For the rest of this report set

$$P = P(RL, R) = P(RL, L)^{-1}$$

and

$$C = C_{RL}(L) \text{ and } \mathbf{C} = \mathbf{C}_{RL}(L).$$

$$PF(RL)\mathbf{u}^{RL} = \mathbf{C}F(L)\mathbf{u} = \begin{bmatrix} F(L)\mathbf{u} \\ CF(L)\mathbf{u} \\ \vdots \\ C^{R-1}F(L)\mathbf{u} \end{bmatrix}.$$

Segmenting $PF(RL)\mathbf{u}^{RL}$ into R contiguous segments of size L, the first segment is $F(L)\mathbf{u}$, while the remaining segments are filtered versions of $F(L)\mathbf{u}$.

Segmenting

$$PZ_{RL}\mathbf{x}^{RN} = \mathbf{C}Z_L\mathbf{x} = \begin{bmatrix} Z_L\mathbf{x} \\ CZ_L\mathbf{x} \\ \vdots \\ C^{R-1}Z_L\mathbf{x} \end{bmatrix},$$

into R contiguous segments of size $L \times K$, the first segment is $Z_L\mathbf{x}$, while the remaining segments are filtered versions of $Z_L\mathbf{x}$.

9 Zero-padded Discrete Chirps

We continue using the notation $P = P(RL, R)$, $C = C_{RL}(L)$ and $\mathbf{C} = \mathbf{C}_{RL}(L)$.

The problem of computing the $RL \times K$ FZT of a zero-padded vector $\mathbf{x}^{RN}$, $\mathbf{x} \in \mathbf{C}^N$, can be reduced to that of computing $Z_L\mathbf{x}$ and then placing $Z_L\mathbf{x}$ into the matrix construction

$$PZ_{RL}\mathbf{x}^{RN} = \mathbf{C}Z_L\mathbf{x}.$$

We can now compute the $RL \times K$ FZT of the zero-padded discrete chirp.

Suppose $\mathbf{x}$ is a discrete chirp. The vector $\mathbf{x}^{RN}$ is called a *zero-padded discrete chirp.*

Since circulant matrices commute we can write

$$\mathbf{C}C_0 = \begin{bmatrix} C_0 \\ C_0C \\ \vdots \\ C_0C^{R-1} \end{bmatrix}.$$

In the segment of $RL \times K$ Zak space formed by the first L rows, the support of $PZ_{RL}\mathbf{x}^{RN}$ is $E_K^L(0)$, while in the remaining segments we 'fill' the segments through the actions of C^r, $1 \leq r < R$.

Similar arguments can be used to derive flexible size FZT's.

10 Windowed Linear Shifts

One of the advantages of representing an echo in Zak space is that the echo can be viewed through different time-frequency windows in Zak space. Knowledge of the shifts making up the echo can be used to define windows through which the echo can be more easily analyzed. Localized, in time-frequency, noise can be rejected by choosing a window avoiding the noisy region. For waveforms having a specific geometric structures when viewed through a window, echo analysis and noise reduction can best proceed by restricting the echo to this window.

The formula

$$PZ_{RL}\mathbf{x}^{RN} = \mathbf{C}Z_L\mathbf{x}, \quad \mathbf{x} \in \mathbf{C}^N,$$

is the starting point for studying the Zak space representation of the shifts

$$S_{RN}^m\mathbf{x}^{RN}, \quad 0 \leq m < (R-1)N.$$

The main result shows that the restriction of $PZ_{RL}S_{RN}^m\mathbf{x}^{RN}$ to the first L rows of $LR \times K$ Zak space is $Z_LS_N^m\mathbf{x}$, $0 \leq m < (R-1)N$. The problem raised by restricting attention to these first L rows of $LR \times K$ Zak space is that ambiguities are raised by the inability to distinguish between the vectors

$$S_{RN}^{n+rN}\mathbf{x}^{RN}, \quad 0 \leq r < R,$$

for fixed $0 \leq n < N$.

For $\mathbf{x} \in \mathbf{C}^N$, set

$$Z_L\mathbf{x} = [X_0\, X_1\, \cdots\, X_{K-1}] \text{ and } Z_{RL}\mathbf{x}^{RN} = [Y_0\, Y_1\, \cdots\, Y_{K-1}].$$

Then

$$Z_{RL}\left(S_{RN}\mathbf{x}^{RN}\right) = \left[D_{RL}Y_{K-1}\,Y_0\,\cdots\,Y_{K-2}\right].$$

Since

$$\mathbf{C}X_k = PY_k, \quad 0 \le k < K,$$

we have

$$PZ_{RL}\left(S_{RN}\mathbf{x}^{RN}\right) = \left[\left(PD_{RL}P^{-1}\right)\mathbf{C}X_{K-1}\,\mathbf{C}X_0\,\cdots\mathbf{C}X_{K-2}\right]$$

where

$$PD_{RL}P^{-1} = \begin{bmatrix} D_L & & & & \\ & \tau D_L & & & \\ & & \cdot & & \\ & & & \cdot & \\ & & & & \tau^{R-1}D_L \end{bmatrix}, \quad \tau = e^{2\pi i\frac{1}{RL}}.$$

As a consequence the restriction of $PZ_{RL}\left(S_{RN}\mathbf{x}^{RN}\right)$ to the first L rows of $RL \times K$ Zak space is

$$Z_L\left(S_N\mathbf{x}\right) = \left[D_L\,X_{K-1}\,X_0\,\cdots\,X_{K-2}\right].$$

The relationship between the remaining rows of

$$PZ_{RL}\left(S_{RN}^m\mathbf{x}^{RN}\right) \text{ and } Z_L\left(S_N^m\mathbf{x}\right)$$

is more complicated due to the lack of commutativity between the FT and shift operations. In Section 12 we develop this relationship, but as yet the results have not proved useful in echo analysis.

Set

$$W_0 = \{(l,k) : 0 \le l < L,\, 0 \le k < K\}.$$

For $\mathbf{y} \in \mathbf{C}^{RN}$

$$W_0PZ_{RL}\mathbf{y}$$

is the $L \times K$ image formed by restricting $PZ_{RL}\mathbf{y}$ to W_0. $W_0PZ_{RL}\mathbf{y}$ is a view of $\mathbf{y}$ through the time-frequency *window* W_0.

$$W_0PZ_{RL}\left(S_{RN}^m\mathbf{x}^{RN}\right) = Z_L\left(S_N^m\mathbf{x}\right),$$

and

$$W_0PZ_{RL}\left(S_{RN}^{m+N}\mathbf{x}^{RN}\right) = W_0PZ_{RL}\left(S_{RN}^m\mathbf{x}^{RN}\right), \quad 0 \le m < (R-1)N.$$

11 Windowed Echos of Zero-padded Discrete Chirps

Suppose $\mathbf{x} \in \mathbf{C}^N$ is a discrete chirp. In Section 12 we show that the set

$$\{PZ_{RL}\left(S_{RN}^r\mathbf{x}^{RN}\right) : 0 \le r < N\}$$

is not orthogonal, but the set

$$W_0 P Z_{RL}\left(S_{RN}^r \mathbf{x}^{RN}\right) = Z_L\left(S_N^r \mathbf{x}\right), \quad 0 \le r < N,$$

is orthogonal and the expansion

$$W_0 P Z_{RL}\mathbf{e} = \sum_{r=0}^{N-1}\left(\sum_{s=0}^{R-2}\alpha(r+sN)\right) Z_L S_N^r \mathbf{x}$$

of an echo $\mathbf{e}$ of $\mathbf{x}^{RN}$ is an orthogonal expansion. The coefficients

$$\sum_{s=0}^{R-2}\alpha(r+sN), \quad 0 \le r < N,$$

can be computed by inner products. If the echo $\mathbf{e}$ has the form

$$\mathbf{e} = \sum_{r=0}^{N-1}\alpha(r) S_{RN}^r \mathbf{x}^{RN},$$

there is no aliasing of the coefficients, and we can compute the coefficients of the echo from the orthogonal expansion

$$W_0 P Z_{RL}\mathbf{e} = \sum_{r=0}^{N-1}\alpha(r) Z_L S_N^r \mathbf{x},$$

by inner products. As in Section 6 dechirping can simplify echo analysis.

An echo of the form

$$\mathbf{e} = \sum_{r=0}^{N-1}\alpha(r) S_{RN}^{r+r_0 N}\mathbf{x}^{RN}$$

looks the same through the window W_0 for all integers r_0. r_0 can be determined from application, from an estimate of the starting time of the echo and potentially, from several size FZT computations of the echo.

Define the *N-periodic multiplication dechirping* operator $M_{\mathbf{x}^*}^{(RN)}$ by

$$M_{\mathbf{x}^*}^{(RN)} = I_R \otimes M_{\mathbf{x}^*} = \begin{bmatrix} M_{\mathbf{x}^*} & & & \\ & \cdot & 0 & \\ & & \cdot & \\ & 0 & & \cdot \\ & & & M_{\mathbf{x}^*} \end{bmatrix}.$$

Write

$$m = r + sN, \quad 0 \le r < N,\ 0 \le s < R-1.$$

Then

$$M_{\mathbf{x}^*}^{(RN)} S_{RN}^m \mathbf{x}^{RN} = S_{RN}^{sN} M_{\mathbf{x}^*}^{(RN)} S_{RN}^r \mathbf{x}^{RN}.$$

N replaced by RN and L replaced by RL implies

$$Z_{RL}\left(S_{RN}^{sN}\mathbf{y}\right) = D_{RL}^{sL} Z_{RL}\mathbf{y},$$

and

$$W_0 PZ_{RL}\left(S_{RN}^{sN}\mathbf{y}\right) = W_0 PZ_{RL}\mathbf{y}, \quad \mathbf{y} \in \mathbf{C}^{RN}.$$

Recall

$$PD_{RL}^{sL}P^{-1} = \begin{bmatrix} I_L & & & \\ & \tau^s I_L & & \\ & & \ddots & \\ & & & \tau^{s(R-1)} I_L \end{bmatrix}, \quad \tau = e^{2\pi i \frac{1}{RL}}.$$

Combining these results we have

$$W_0 PZ_{RL}\left(M_{\mathbf{x}^*}^{(RN)} S_{RN}^m \mathbf{x}^{RN}\right) = W_0 PZ_{RL}\left(M_{\mathbf{x}^*}^{(RN)} S_{RN}^r \mathbf{x}^{RN}\right).$$

Since $0 \le r < N$,

$$M_{\mathbf{x}^*}^{(RN)} S_{RN}^r \mathbf{x}^{RN} = S_{RN}^r \left(\left(S_N^{-1}\mathbf{x}^*\right)\mathbf{x}\right)^R,$$

and

$$W_0 PZ_{RL}\left(M_{\mathbf{x}^*}^{(RN)} S_{RN}^m \mathbf{x}^{RN}\right) = Z_L\left(M_{\mathbf{x}^*} S_N^r \mathbf{x}\right).$$

Consider the echo

$$\mathbf{e} = \sum_{m=0}^{(R-1)N-1} \alpha(m) S_{RN}^m \mathbf{x}^{RN}.$$

Dechirping $\mathbf{e}$ and operating by $W_0 PZ_{RL}$ we have

$$W_0 PZ_{RL}\left(M_{\mathbf{x}^*}^{(RN)}\mathbf{e}\right) = L\sum_{r=0}^{N-1}\left(\sum_{s=0}^{R-2}\alpha(r+sN)\right) x(-r) F_K^L(r) D_N^{-r}(K).$$

Special echoes can be handled exactly as before in Section 6.

The W_0-window is emphasized in this report but there are other windows with potential applications.

12 Linear Shifts

In this section we study the relationship between

$$PZ_{RL}\left(S_{RN}^m \mathbf{x}^{RN}\right) \text{ and } Z_L\left(S_N^m \mathbf{x}\right)$$

over complete $RL \times K$ Zak space. The results are technical and have as yet not been applied to echo analysis. The presentation will be brief with several derivations omitted.

In Section 10 we showed that

$$PZ_{RL}\left(S_{RN}\mathbf{x}^{RN}\right) = \left[\mathbf{D}\mathbf{C}X_{K-1}\ \mathbf{C}X_0\ \cdots\ \mathbf{C}X_{K-2}\right],$$

where $\mathbf{D}$ is the $RL \times RL$ diagonal matrix

$$\mathbf{D} = PD_{RL}P^{-1} = \begin{bmatrix} D_L & & & & \\ & \tau D_L & 0 & & \\ & & \cdot & & \\ & & & \cdot & \\ & & 0 & & \cdot \\ & & & & \tau^{R-1}D_L \end{bmatrix}, \quad \tau = e^{2\pi i \frac{1}{RL}}.$$

For the remainder of this section,

$$m = r + sN, \quad 0 \le r < N, \ 0 \le s < R,$$

and

$$r = t + uL = a + bK, \quad 0 \le t, \ b < L, \ 0 \le u, \ a < K.$$

For $0 \le b \le L$, define the vector $\mathbf{f}_b^L \in \mathbf{C}^L$ by

$$\mathbf{f}_b^L = \begin{bmatrix} \mathbf{1}^b \\ \mathbf{0}^{L-b} \end{bmatrix},$$

and the $L \times L$ circulant matrix $C(b)$ by

$$C(b) = F(L)D\left(\mathbf{f}_b^L\right)F(L)^{-1}.$$

The difficulty in studying the shifts

$$S_{RN}^m \mathbf{x}^{RN}, \quad 0 \le m < (R-1)N,$$

by their $RL \times K$ Zak space representations is due to the noncommutativity of D_L and C. D_L and S_L do not commute!

Define the vector $\mathbf{g}_b^L \in \mathbf{C}^L$ by

$$\mathbf{g}_b^L = \begin{bmatrix} \mathbf{0}^b \\ \mathbf{1}^{L-b} \end{bmatrix}, \quad 0 \le b \le L.$$

The vectors $M_k(b) \in \mathbf{C}^L$,

$$M_k(b) = C(b)D_L^b X_k, 0 \le k < K,$$

are the blurring factors.

Suppose $\mathbf{x} \in \mathbf{C}^N$ is a discrete chirp. Expanding

$$C(b) = \frac{1}{L}\sum_{c=0}^{b-1} D_L^c \left(\mathbf{1}^L \otimes \left(\mathbf{1}^L\right)^t\right) D_L^{-c},$$

and

$$M_k(b) = x(k)\sum_{c=0}^{b-1} v^{-(b-c)k} D_L^c \mathbf{1}^L$$

and placing this result in

$$PZ_{RL}\left(S_{RN}^{r}\mathbf{x}^{RN}\right) = \mathbf{D}^{b}\left[\mathbf{D}\mathbf{C}X_{K-a}\cdots\mathbf{D}\mathbf{C}X_{K-1}\,\mathbf{C}X_{0}\cdots\mathbf{C}X_{K-a-1}\right].$$

The term

$$\mathbf{z}\mathbf{C}M_{L}(a,b)$$

is the problem. It is responsible for obstructing the construction of a zero-padded discrete chirp whose linear shifts form an orthogonal set. In fact we can show that the inner product

$$\langle PZ_{RL}\mathbf{x}^{RN}, PZ_{RL}\left(S_{RN}\mathbf{x}^{RN}\right)\rangle$$

is not zero. This inner product is

$$\langle \mathbf{C}Z_{L}\mathbf{x}, \mathbf{C}Z_{L}\left(S_{N}\mathbf{x}\right)\rangle + \langle \mathbf{C}Z_{L}\mathbf{x}, \mathbf{z}\mathbf{C}M_{L}(1,0)\rangle.$$

The first inner product vanishes. Since

$$M_{L}(1,0) = \left[M_{K-1}(1)\,\mathbf{0}^{L}\,\cdots\,\mathbf{0}^{L}\right],$$

the second inner product is

$$\sum_{c=0}^{R-1} Z_{c}\langle X_{0}, M_{K-1}(1)\rangle = -R\langle X_{0}, M_{K-1}(1)\rangle.$$

From

$$M_{K-1}(1) = vx(1)\mathbf{1}^{L},$$

we have

$$\langle X_{0}, M_{K-1}(1)\rangle = Lv^{-1}x^{*}(1),$$

and

$$\langle PZ_{RL}\mathbf{x}^{RN}, PZ_{RL}\left(S_{RN}\mathbf{x}^{RN}\right)\rangle = -RLv^{-1}x^{*}(1) \neq 0.$$

13 Filtering Algorithms

The algorithms of Section 11 are based on windowing the $RL \times K$ Zak transform of an echo $\mathbf{e}$. In this section a more complex filtering of this Zak space image will be introduced. Surprisingly, perhaps, the resulting algorithm has simple structure. The range of applications is the same as that handled by the W_0-window algorithm. The eventual goal is to combine these approaches in a multiple chirp interrogation of a general target scene.

For $\mathbf{y} \in \mathbf{C}^{RN}$, write

$$\mathbf{y} = [\mathbf{y}_{s}]_{0\leq s<R}, \quad \mathbf{y}_{s} \in \mathbf{C}^{N}, \;\; 0 \leq s < R.$$

The basic idea underlying the approach in this section is to segment an echo

$$\mathbf{y} = \sum_{m=0}^{RN-1} \alpha(m) S_{RN}^{m}\mathbf{x}^{RN}, \quad \mathbf{x} \text{ a discrete chirp},$$

into the R segments

$$\mathbf{y}_s \in \mathbf{C}^N, \quad 0 \le s < R,$$

and then to compute the FZT of each segment

$$Z_L\mathbf{y}_s, \quad 0 \le s < R.$$

Under certain conditions the coefficients of $\mathbf{y}$ can be computed by first computing the sums

$$Z_L\mathbf{y}_s + Z_L\mathbf{y}_{s+1}, \quad 0 \le s < R,$$

and then applying the methods of the preceding sections.

Suppose $\mathbf{y} \in \mathbf{C}^{RN}$. The first result relates $Z_{RL}\mathbf{y}$ to the FZT of the segments of $\mathbf{y}$

$$Z_L\mathbf{y}_s, \quad 0 \le s < R.$$

First observe that

$$M_{RL}\mathbf{y} = [M_L y_r]_{0 \le r < R}.$$

and

$$PZ_{RL}\mathbf{y} = PF(RL)M_{RL}\mathbf{y} = PF(RL)\left[M_L\mathbf{y}_r\right]_{0 \le r < R}. \tag{2}$$

The RL CT FFT factorization will be used to compute $PZ_{RL}\mathbf{y}$ in terms of $Z_L\mathbf{y}_s$, $0 \le s < R$.

Set

$$\mathbf{C}^* = \frac{1}{R}\left[I_L\, C^{-1} \cdots C^{-(R-1)}\right]$$

and

$$\mathbf{F} = \left(F(R)^{-1} \otimes I_L\right)\mathbf{C}^*.$$

$\mathbf{F}$ can be viewed as a Zak space filtering operation.

As before we write

$$m = r + sN, \quad 0 \le r < N, \;\; 0 \le s < R,$$

and

$$r = a + bK = t + uL, \quad 0 \le a,\, u < K, \;\; 0 \le b,\, t < L$$

and suppose $\mathbf{x}$ is a discrete chirp satisfying the $L \times K$ Zak space condition.

$$\mathbf{F}PZ_{RL}\left(S_{RN}^m\mathbf{x}^{RN}\right) = \left(F(R)^{-1} \otimes I_L\right)\left(\mathbf{D}^{sL}Z_L\left(S_N^r\mathbf{x}\right) + \mathbf{z}\mathbf{D}^{sL}M_L(a,b)\right).$$

Since

$$\left(F(R)^{-1} \otimes I_L\right)\mathbf{D}^{sL} = \mathbf{e}_s^R \otimes I_L$$

and

$$\left(F(R)^{-1} \otimes I_L\right)\left(\mathbf{z}\mathbf{D}^{sL}\right) = -\mathbf{e}_s^R \otimes I_L + \mathbf{e}_{s+1}^R \otimes I_L.$$

we have the following.

Suppose $\mathbf{y}$ is an echo of the form

$$\mathbf{y} = \sum_{r=0}^{N-1} \alpha(r+sN) S_{RN}^{r+sN} \mathbf{x}^{RN},$$

for fixed $0 \le s < R$. Then

$$Z_L \mathbf{y}_s = \sum_{r=0}^{R-1} \alpha(r+sN) \left(Z_L \left(S_N^r \mathbf{x} \right) - M_L(a,b) \right),$$

$$Z_L \mathbf{y}_{s+1} = \sum_{r=0}^{R-1} \alpha(r+sN) M_L(a,b)$$

and

$$Z_L \mathbf{y}_{s'} = \mathbf{0}^N, \quad s' \neq s, \text{ or } s' \neq s+1.$$

Then

$$\sum_{r=0}^{N-1} \alpha(r+sN) Z_L \left(S_N^r \mathbf{x} \right) = Z_L \mathbf{y}_s + Z_L \mathbf{y}_{s+1}$$

and we can compute the coefficients of $\mathbf{y}$ by the previous methods from the sum

$$Z_L \mathbf{y}_s + Z_L \mathbf{y}_{s+1}.$$

The same argument shows that for echoes of the forms

- $\mathbf{y} = \sum_{r=0}^{N-1} \alpha(r+sN) S_{RN}^{r+sN} \mathbf{x}^{RN}$, for fixed $0 \le s < R$.
- $\mathbf{y} = \sum_{r=0}^{N-1} \alpha(r+s_1N) S_{RN}^{r+s_1N} \mathbf{x}^{RN} + \sum_{r=0}^{N-1} \alpha(r+s_2N) S_{RN}^{r+s_2N} \mathbf{x}^{RN}$, for fixed $0 \le s_1, s_2 < R$, with $|s_1 - s_2| \ge 2$
- $$\mathbf{y} = \sum_{j=1}^{R_1} \sum_{r=0}^{N-1} \alpha\left(r + s_j N\right) S_{RN}^{r+s_j N} \mathbf{x}^{RN}, \text{ for fixed } 0 \le s_1 < s_2 < \cdots < s_{R_1} < R$$

  where $|s_j - s_{j+1}| \ge 2$, $1 \le j < R_1$,

the coefficients of the echoes can be computed by the methods of the preceding sections from the sums

$$Z_L \mathbf{y}_s + Z_L \mathbf{y}_{s+1}, \quad 0 \le s < R.$$

However if echo $\mathbf{y}$ has the form

$$\mathbf{y} = \sum_{r=0}^{N-1} \alpha(r) S_{RN}^r \mathbf{x}^{RN} + \sum_{r=0}^{N-1} \alpha(r+N) S_{RN}^{r+N} \mathbf{x}^{RN},$$

then

$$Z_L \mathbf{y}_1 = \sum_{r=0}^{N-1} \alpha(r) M_L(a,b) + \sum_{r=0}^{N-1} \alpha(r+N) \left(Z_L \left(S_N^r \mathbf{x} \right) - M_L(a,b) \right), \quad r = a + bK,$$

from which we see that the information containing the coefficients of the first sum to that of the second sum cannot be decoupled.

14 Material Identification in Zak Space

In a previous report [1] we developed algorithms for numerically deconvolving Krueger's formula

$$e_a(t) = \int_{-\infty}^{t} \rho_a(t-u) x_a^T(u) du, \quad t \in \mathbb{R},$$

relating the reflectivity kernel ρ_a of a dielectric material to the echo e_a resulting from the interaction of an orthogonally incident chirp x_a^T with the material. The goal in this section is to describe a new deconvolution algorithm using the Zak space framework developed in the preceding sections.

Assume throughout that ρ_a is supported in an interval $[0, J)$, J estimated in some range but not known and x_a^T a waveform supported on the interval $[0, T)$. The echo e_a is then supported in the interval $[0, T + J)$. Until required we do not assume that x_a^T is a chirp.

Choose an integer R satisfying the condition

$$J < RT.$$

If there are several possible materials under investigation, we can choose R sufficiently large so that this condition holds for all the estimated J's.

The expression for the echo will be discretized. Choose a positive integer N and set $M = NR$. Approximate the integral by the Riemann sum corresponding to the points

$$\frac{m}{M} RT = \frac{m}{N} T, \quad 0 \le m < M,$$

with the resulting approximation

$$e_a(t) = \frac{T}{N} \sum_{m=0}^{M-1} \rho_a\left(\frac{m}{N}T\right) x_a^T\left(t - \frac{m}{N}T\right), \quad t \in \mathbb{R}.$$

Sample the echo at the points

$$\frac{n}{M} RT, \quad 0 \le n < (R+1)N,$$

with the resulting approximation

$$e_a\left(\frac{n}{N}T\right) = \frac{T}{N} \sum_{m=0}^{M-1} \rho_a\left(\frac{m}{N}T\right) x_a^T\left(\frac{n-m}{N}T\right), \quad 0 \le n < (R+1)N.$$

Setting

$$\mathbf{x} = \left[x_a^T\left(\frac{m}{N}T\right)\right]_{0 \le m < N}, \quad \mathbf{e} = \left[e_a\left(\frac{n}{N}T\right)\right]_{0 \le n < (R+1)N},$$

and

$$\rho(m) = \rho_a\left(\frac{m}{N}T\right), \quad 0 \le m < M,$$

the approximation can be written

$$\mathbf{e} = \frac{T}{N} \sum_{m=0}^{M-1} \rho(m) S^m_{(R+1)N} \mathbf{x}^{RN}.$$

$\mathbf{e}$ is an echo of the zero-padded vector $\mathbf{x}^{(R+1)N}$, $\mathbf{x} \in \mathbf{C}^N$.

In applications it sometimes useful to modify the discretization by sampling the integral at the points

$$\frac{m}{N}T, \quad 1 \le m \le M,$$

and the echo at the points

$$\frac{n}{N}T, \quad 1 \le n \le (R+1)N,$$

with the resulting approximation

$$e_a\left(\frac{n}{N}T\right) = \frac{T}{N} \sum_{m=1}^{M} \rho\left(\frac{m}{M}T\right) x_a^T\left(\frac{n-m}{N}T\right), \quad 1 \le n \le (R+1)N.$$

By the change of variables

$$m' = m - 1 \text{ and } n' = n - 1,$$

$$e_a\left(\frac{n'+1}{N}T\right) = \frac{T}{N} \sum_{m'=0}^{M-1} \rho_a\left(\frac{m'+1}{N}T\right) x_a^T\left(\frac{n'-m'}{N}T\right).$$

Setting

$$\mathbf{x} = \left[x_a^T\left(\frac{m}{N}T\right)\right]_{0 \le m < N}, \quad \mathbf{e} = \left[e_a\left(n\frac{T}{N}\right)\right]_{1 \le n \le (R+1)N},$$

and

$$\rho(m) = \left[\rho_a\left(\frac{m}{N}T\right)\right]_{1 \le m < M},$$

we have

$$\mathbf{e} = \frac{T}{N} \sum_{m=0}^{M-1} \rho(m+1) S^m_{(R+1)N} \mathbf{x}^{(R+1)N}.$$

The second sampling is preferred whenever we want to avoid ρ_a at the origin.

Methods for analyzing such echoes in Zak space were discussed in the preceding section when x_a^T is a chirp

$$x_a^T(t) = \begin{cases} e^{\pi i \gamma t^2} e^{2\pi i \beta t}, & 0 \le t < T, \\ 0, & \text{otherwise}, \end{cases} \qquad t \in \mathbf{R},$$

such that

$$N = \gamma T^2$$

is a positive integer and the periodic modulo N condition holds.

$$e^{\pi i N} e^{2\pi i \beta t} = 1.$$

Assume for the rest of this report that a chirp x_a^T satisfies these two conditions.

Suppose now that x_a^T is a chirp in the formula

$$\mathbf{e} = \frac{T}{N} \sum_{m=0}^{(R_1-1)N-1} \rho(m) S_{R_1 N}^m \mathbf{x}^{RN}, \quad R_1 = R+1,$$

derived above. Set $N = LK$. Windowing to the first L rows of $R_1 L \times K$ Zak space, we have that the expansion

$$W_0 P Z_{R_1 L} \mathbf{e} = \frac{T}{N} \sum_{m=0}^{(R_1-1)N-1} \rho(m) Z_L S_N^m \mathbf{x}, \quad P = P(R_1 L, R_1),$$

is an orthogonal expansion after collecting like powers of S_N and we can compute the sums

$$\sum_{s=0}^{R_1-1} \rho(r+sN), \quad 0 \le r < N,$$

by inner products.

For sufficiently large T we can in the absence of noise compute the scattering coefficients themselves. Suppose

$$J < T$$

and we take $R = 1$. Windowing to the first L rows in $2L \times K$ Zak space

$$W_0 P(2L, 2) Z_{2L} \mathbf{e} = \frac{T}{N} \sum_{m=0}^{N-1} \rho(m) Z_L S_N^m \mathbf{x}$$

is an orthogonal expansion and we can compute the $\rho(m)$, $0 \le m < N$, by inner products.

Figures 17 – 19 illustrates this orthogonality. In Figure 19, usual matched filter processing result is also displayed and compared. Note that the matched filter processing is over the entire space and orthogonality is lost. The relevant parameters for these figures are $J = 10$, $T = 20$, $R = 1$, $\gamma = .25$ and $f = 20$. The Zak transform parameters are $L = 10$ and $K = 10$. Figures 20 and 21 display equivalent information in the presence of noise.

Figure 17: Test reflectivity kernel

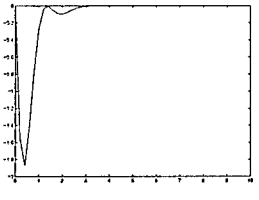

Suppose N has factorization $N = LK$ such that

$$J < \frac{T}{K}.$$

Figure 18: Sampled echo from discrete chirp pulse upon interrogating the test material

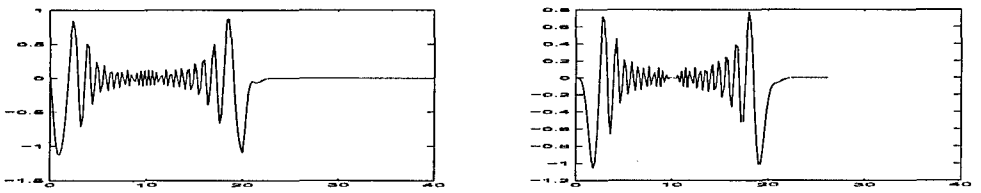

real part imaginary part

Figure 19: Recovered reflectivity kernels

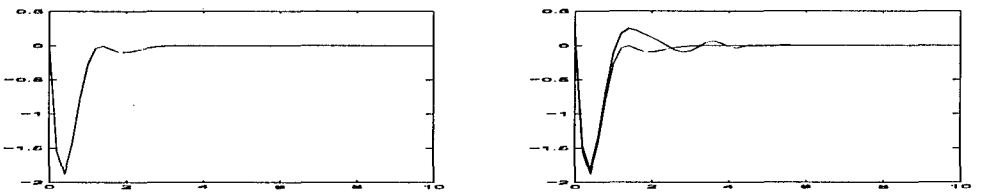

windowed inner products matched filter processing

In $2L \times K$ Zak space

$$W_0 P(2L,2) Z_{2L} \mathbf{e} = \frac{T}{N} \sum_{m=0}^{L-1} \rho(m) Z_L S_N^m \mathbf{x}.$$

The supports of the terms of the summation

$$\rho(m) Z_L S_N^m \mathbf{x}, \quad 0 \le m < L,$$

are pairwise disjoint lines in $L \times K$ space. $|\rho(m)|$ is the common absolute value at each point of the line

$$E_K^L(m), \quad 0 \le m < L.$$

For a noisy echo we can estimate $|R(m)|$ from the possibly varying absolute values on the line.

For the chirp pulse the integral is approximated by a Riemann sum corresponding to the points

$$\frac{m}{M} RT = \frac{m}{N} T = m \frac{1}{\gamma T}, \quad 0 \le m < M.$$

The larger we take γT, the finer the sampling grid, and the better the approximation. The same is true for the reflectivity kernel samples $\rho(m)$, $0 \le m < M$.

Figures 23 and 24 are included to illustrate how the Zak space representations reflect the effective supports of the reflectivity kernels.

Figure 20: Sampled noisy echo

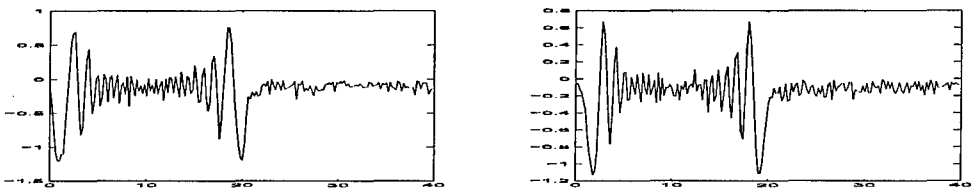

real part imaginary part

Figure 21: Recovered reflectivity kernel using windowed inner products

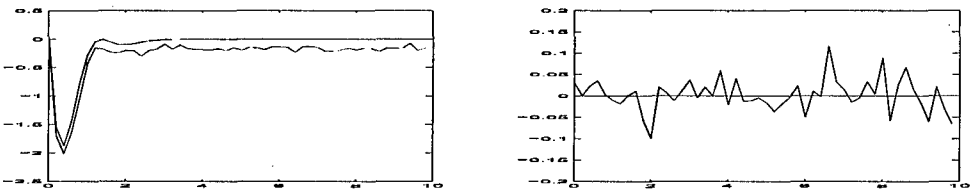

real part imaginary part

Simplest denoising in Zak domain is used to estimate the reflectivity kernel coefficients in the presence of noise. The number of lines in the Zak space representation of the echo is determined, then the values along each line are averaged. Figures 25 – 27 display the results of denoising. Zak transform parameters are $L = 40$ and $K = 40$.

Setting $L = 20$, we have another estimate for the first 20 coefficients of the reflectivity kernel. The comparison between these estimates are displayed against the test kernel in figure 32. The first plot is that of the estimate from using $L = 40$. The second plot is the estimate from using $L = 20$. The last is the average of the two sets of the estimates.

There is a second approach which potentially increases the accuracy of the integral approximation and provide better resolution for the reflectivity kernel samples. As before

$$J < RT.$$

Choose any positive integer K and set $M = RNK$. Sampling the integral and the echo at the points

$$\frac{n}{M}RT = \frac{n}{KN}T,$$

we have the approximation

$$e_a\left(\frac{n}{KN}T\right) = \frac{T}{KN}\sum_{m=0}^{M-1}\rho_a\left(\frac{m}{KN}\right)x_a^T\left(\frac{n-m}{KN}T\right), \quad 0 \le n < (R+1)KN.$$

Figure 22: Recovered reflectivity kernel using matched filter processing

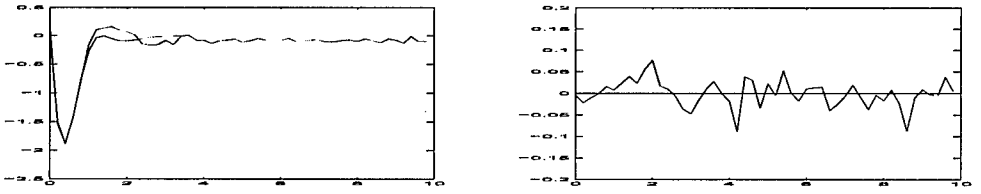

real part imaginary part

Figure 23: Test reflectivity kernel and the Zak transform of the echo

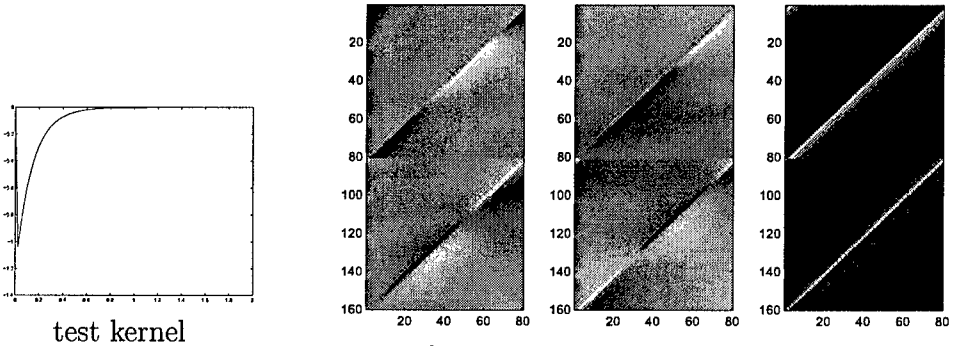

test kernel real part imaginary part absolute value

The sequence

$$x(n) = x_a^T\left(\frac{n}{KNT}\right), \quad n \in \mathbf{Z},$$

where x_a^T is a chirp is the oversampled chirp in Section 2. Future work will study the Zak space structure of oversampled chirps, shifts and echoes.

15 Atmospheric Effects

15.1 Introduction

In this section we begin a preliminary investigation into the effects of atmospheric interference on a waveform interrogating a ground based dielectric material from a space-based radar. We propose two multiple measurement strategies for removing this interference by singular value decomposition methods. In future work we plan to study methods based more significantly on the electromagnetic differences between the atmosphere as a magnetically biased plasma and an interrogated dielectric material.

Figure 24: Test reflectivity kernel and the Zak transform of the echo

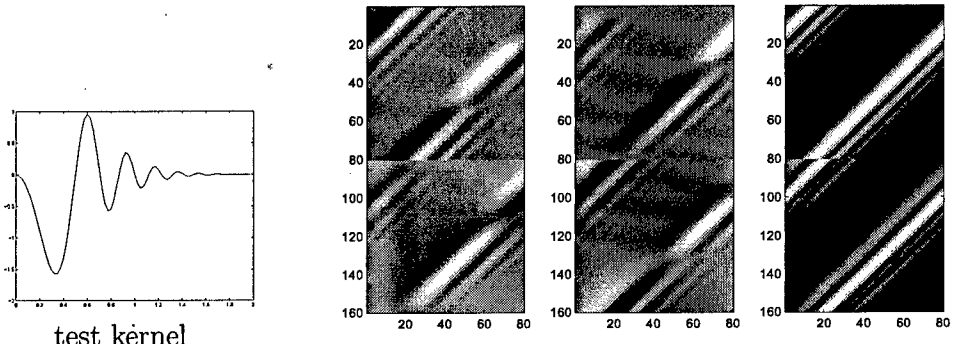

Figure 25: Noise-free echo

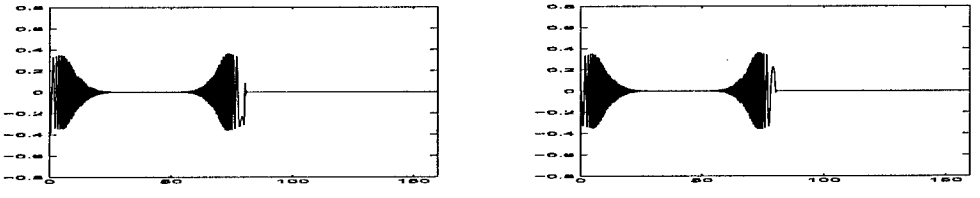

Throughout this section atmospheric interference is modeled as a linear convolution. Suppose a pulse x_a is transmitted from a space-based radar, passes through atmospheric interference modeled as a linear convolution with an impulse response function h_1, interrogates a dielectric material having reflectivity kernel ρ_a and returns through atmospheric interference now modeled by an impulse response function h_2. Suppressing signal translation due to travel time the echo e_a is the triple convolution

$$e_a(t) = \int h_2(w) \int \rho_a(v) \int h_1(u) x_a(t - w - v - u) du\, dv\, dw.$$

By Fubini's theorem we can under natural assumptions on the waveforms in the triple convolution interchange orders of integration and write

$$e_a(t) = \int (h_2 * h_1)(r)(\rho_a * x_a)(t - r) dr,$$

where

$$h(r) = (h_2 * h_1)(r) = \int h_2(w) h_1(r - w) dw$$

Figure 26: Noise-added echo

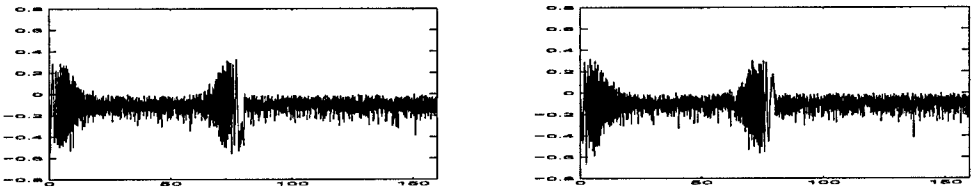

real part imaginary part

Figure 27: Test and estimated reflectivity kernel

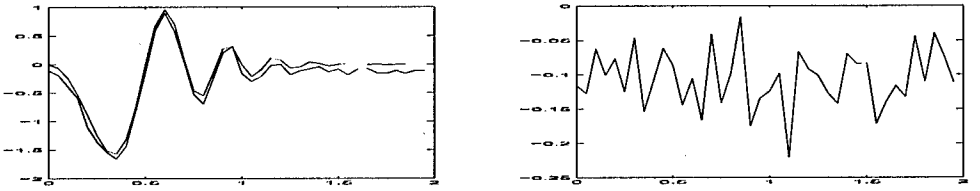

real part imaginary part

and

$$\rho_a * x_a(t) = \int \rho_a(v) x_a(t-v) dv.$$

Suppose

$$supp\, \rho_a \subset [0, T)$$

and that R_1 and R_2 are integers such that

$$supp \rho_a \subset [0, R_1 T)$$

and

$$supp\, h \subset [0, R_2 T).$$

The echo e_a is supported in the interval

$$[0, RT), \quad R = R_1 + R_2 + 1$$

and

$$e_a(t) = \int_0^{R_2 T} h(r) \left(\rho_a * x_a\right)(t-r) dr, \quad t \in \mathbf{R},$$

where

$$\left(\rho_a * x_a\right)(t) = \int_0^{R_1 T} \rho_a(u) x_a(t-u) du, \quad t \in \mathbf{R}.$$

Figure 28: Noise-added echo

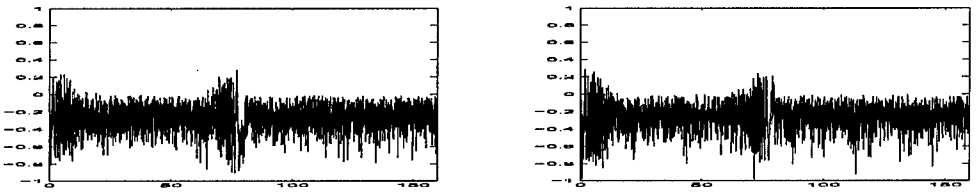

real part imaginary part

Figure 29: Test and estimated reflectivity kernel

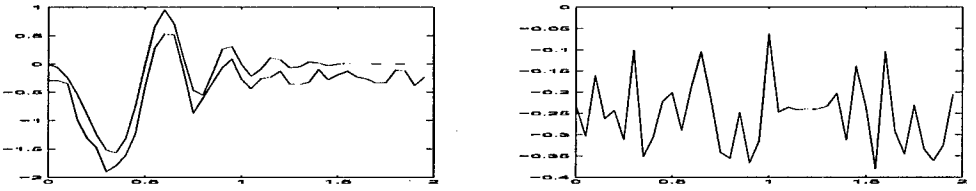

real part imaginary part

Choose a positive integer N and set

$$M_1 = R_1 N,\ M_2 = R_2 N \text{ and } M = RN.$$

Discretizing the integral formula for the echo by

$$r = \frac{m}{M_2} R_2 T = \frac{m}{N} T, \quad 0 \le m < M_2,$$

and

$$t = \frac{n}{M_2} R_2 T = \frac{n}{N} T, \quad 0 \le n < M,$$

we have the approximation

$$e_a\left(\frac{n}{N}T\right) = \frac{T}{N} \sum_{m=0}^{M_2-1} h\left(\frac{m}{N}T\right) (\rho_a * x_a)\left(\frac{n-m}{N}T\right), \quad 0 \le n < M.$$

Discretizing the integral formula for $\rho_a * x_a$ by

$$u = \frac{k}{M_2} R_2 T = \frac{k}{N} T, \quad 0 \le k < M_1,$$

we have the approximation

$$e_a\left(\frac{n}{N}T\right) = \frac{T^2}{N^2} \sum_{m=0}^{M_2-1} h\left(\frac{m}{N}T\right) \sum_{k=0}^{M_1-1} \rho_a\left(\frac{k}{N}T\right) x_a\left(\frac{n-(m+k)}{N}T\right), \quad 0 \le n < RN.$$

Figure 30: Noise-added echo

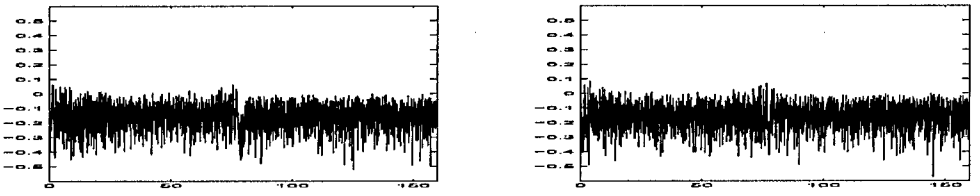

real part imaginary part

Figure 31: Test and estimated reflectivity kernels

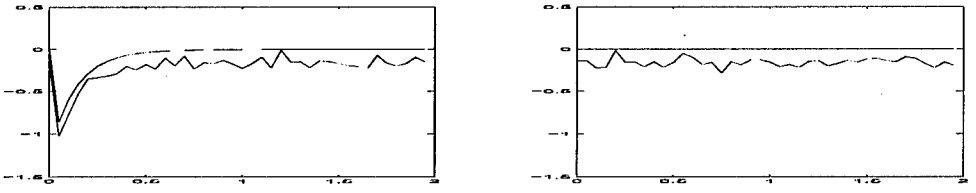

real part imaginary part

Using the notation of the preceding sections with

$$\mathbf{e} = \left[e_a\left(\frac{n}{N}T\right)\right]_{0\le n<RN}, \quad \mathbf{x} = \left[x_a\left(\frac{n}{N}T\right)\right]_{0\le n<N},$$

and

$$\rho(k) = \rho_a\left(\frac{k}{N}T\right),\ 0 \le k < M_1,\ h(m) = h\left(\frac{m}{N}T\right),\ 0 \le m < M_2,$$

we have

$$\mathbf{e} = \frac{T^2}{N^2}\sum_{m=0}^{M_2-1}\sum_{k=0}^{M_1-1} h(m)\rho(k)S_M^{m+k}\mathbf{x}^M.$$

The echo $\mathbf{e}$ is a linear combination of shifts of $\mathbf{x}^M$, however the coefficients are corrupted by the samples of h.

In order to place these formulas within the SVD framework we define the sequences

$$e(n) = e_a\left(\frac{n}{N}T\right),\ n \in \mathbf{Z},\ x(n) = x_a\left(\frac{n}{N}T\right),\ n \in \mathbf{Z},$$

and

$$\rho(k) = \rho_a\left(\frac{k}{N}T\right),\ k \in \mathbf{Z},\ h(m) = h\left(\frac{m}{N}T\right),\ m \in \mathbf{Z}.$$

Figure 32: Test and estimated reflectivity kernels

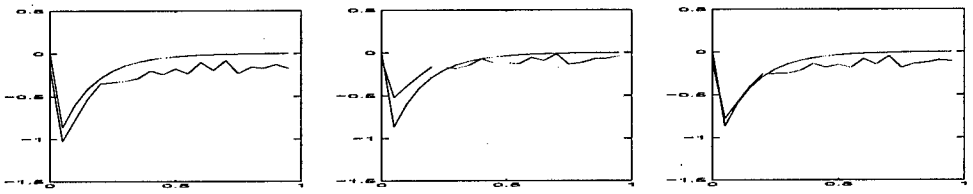

Each sequence is causal and has finite support. The echo e is the triple linear convolution of sequences

$$e = \frac{T^2}{N^2} h * (\rho * x).$$

The problem is to estimate $\rho * x$ from e. Two multiple measurement strategies will be outlined for removing h by SVD methods. These methods are described in detail in the following sections and codes have been implemented. The extensive treatment of these SVD methods can potentially lead to other multiple measurement strategies and multiple waveform strategies for removing atmospheric effects. These strategies will be studied in future work.

15.2 Multiple Measurement Strategies

15.2.1 Strategy 1

We propose two transmissions of the same pulse x_a from a space-based radar with the assumptions that the atmospheric interference h is the same for both transmissions, but the ground region under interrogation is a known dielectric material ρ_1 for the first transmission and an unknown dielectric material ρ_2 for the second transmission. The corresponding echoes are

$$e_1 = h * (\rho_1 * x) \text{ and } e_2 = h * (\rho_2 * x).$$

Set

$$s_1 = \rho_1 * x \text{ and } s_2 = \rho_2 * x.$$

The problem is to compute s_2 with s_1 known.

15.2.2 Strategy 2

We propose two transmissions of the same pulse x_a from a space-based radar interrogating the same dielectric material ρ, but the first passing through atmospheric interference $h = h_1 * h_1$ and the second passing through atmospheric interference $h' = (h_1 + \Delta) * (h_1 + \Delta)$, where Δ is a known perturbation. The corresponding echoes are

$$e = h * (\rho * x), \quad e' = h' * (\rho * x).$$

The problem is to estimate h. As in Strategy 1 if h is computed, we can then compute $\rho * x$.

There are several potentially useful variants of measurement strategies 1 and 2. Different pulses can be transmitted, pulse-trains suitably separated in time can be transmitted. Angle of incidence dependence can be used to distinguish between h and ρ.

16 Future Efforts

To realize the potential of the methods and algorithms developed in this report as tools for material identification we will carry out research leading to algorithms in the following topics.

- Refinement and extension of existing algorithms.
- Waveform design in Zak space.
- Multi-measurements of multiple targets, including the dependence of reflectivity kernels on incident angle.
- Atmospheric effects.

16.1 Refinement and extension of existing algorithms

We identify the following topics for future work

- Varying size FZT representations.
- Windows in Zak space.
- Oversampled chirp pulses.

Throughout this report, a fixed factorization $N = LK$ is taken to represent a discrete waveform (before zero-padding) of size N in $L \times K$ Zak space. For each factorization a noise-free echo of a discrete chirp in Zak space is supported by a series of parallel lines of slope 1, but the aliasing depends on the factorization. We will study how processing the echo relative to several factorizations can be used to remove this aliasing.

In numerical experiments we have seen that echo reconstruction from noisy echoes varies as the factorization varies. It seems that noise is distributed differently for different factorizations of N that is in varying size Zak space representations. We will study this dependence to improve on noise reduction algorithms.

In this report a specific Zak space window W_0 was specified so that through W_0 the collection of linear shifts of a critically sampled zero-padded chirp pulse is orthogonal. However information is lost through the window. The resulting windowed orthogonal expansion of the echo is aliased. We plan to study new windows either subsets of Zak space or unitary transforms of windows in Zak space for removing this aliasing for critically sampled chirp

pulses and more general sampled waveforms. These new windows can also be matched to the noise characteristics in a specific application.

Oversampled chirp pulses were mentioned in the report with a formula relating oversampled chirp pulses to critically sampled chirp pulses. We plan to study the extension of the Zak space framework to oversampled chirp pulses. This effort will provide greater flexibility in the use of Zak space methods to multiple chirp pulses of varying time duration and chirp rates.

16.2 Waveform design

Zak space methods are specially tuned to critically sampled echoes of chirp pulses providing a windowed representation supported on series of parallel lines. We plan to study

- The representation of echoes resulting from more general waveforms, including multiple critically sampled chirp pulses, upchirps and downchirps.
- Waveform design directly in Zak space including lines at varying slopes, polygonal and other geometric structures.

In the second study the inverse Zak transform will be used to construct the appropriate discrete waveform and several methods will be used to construct continuous waveforms and sampling rates supporting these one-dimensional discrete waveforms.

We are especially interested in designing Zak space waveforms which behave well with respect to shifts (lines) and rotations (accelerated targets). Since the Zak space representation of FT is essentially 90° rotation, geometric structures invariant under 90° rotation may be of special interest. In a previous report [1] we use this idea to construct an orthogonal eigen vector basis of the FT having minimal time-frequency support.

16.3 Multiple measurements/multiple targets

In [1] we developed and tested algorithms for distinguishing I_0 stationary dielectric targets along with their reflectivity kernels using J_0 strip SAR measurements from chirp pulse echoes under the assumption that the reflectivity kernels are independent of the incident angle of the interrogating chirp pulses. The results of Section 14 will be used to develop a similar algorithm in the Zak space framework.

As in Section 14 suppose x_a^T is a chirp pulse

$$x_a^T = \begin{cases} e^{\pi i \gamma t^2} e^{2\pi i \beta t}, & 0 \le t < T, \\ 0, & \text{otherwise} \end{cases} \qquad t \in \mathbf{R},$$

satisfying $N = \gamma T^2$ is a positive integer and

$$e^{\pi i N} e^{2\pi i f} = 1, \quad f = \beta T.$$

Assume throughout that the relaxation constant J of all the dielectric materials interrogated satisfy

$$J < T.$$

The formula for the windowed critically sampled echo in Section 14 does not include the shift due to the time traveled between antenna and target. Suppose a chirp x_a^T having carrier frequency β is transmitted from antenna at $\mathbf{v}$ and orthogonally interrogates a dielectric material with reflectivity kernel ρ_a at $\mathbf{u}$. The echo at $\mathbf{v}$ is

$$e_a(t) = \int_0^T \rho_a(t) x_a^T(-u_0 + t - v)dv,$$

where $u_0 = \frac{2}{c}|\mathbf{v} - \mathbf{u}|$. Write

$$u_0 = l_0 \frac{T}{N} + \epsilon_0,$$

where $l_0 \geq 0$ is an integer and $\epsilon < \frac{T}{N}$. Then

$$e_a\left(t + l_0 \frac{T}{N}\right) = \int_0^T \rho_a(v) x_a^T(-\epsilon_0 + (t - v))dv.$$

Sampling the integral at

$$v = \frac{m}{N}T,\ 0 \leq m < N, \text{ and } t = \frac{n}{N}T,\ 0 \leq n < 2N,$$

we have the approximation

$$e_0\left(\frac{n + l_0}{N}T\right) = \frac{T}{N}\sum_{m=0}^{N-1} \rho_a\left(\frac{m}{N}T\right) x_a\left(-\epsilon_0 + \frac{n-m}{N}T\right).$$

If $\epsilon_0 = 0$, we can argue as before to compute the reflectivity kernel samples. We assume the model introduced in 2 that

$$0 \leq \epsilon_0 < \frac{T}{N}$$

and that for $\epsilon_0 > 0$, we can make the approximations

$$x_a^T(-\epsilon_0 + T) = x_a^T(0)e^{-2\pi i\beta\epsilon_0}$$

and

$$x_a^T\left(-\epsilon_0 + \frac{n}{N}T\right) = x_a^T\left(\frac{n}{N}T\right)e^{-2\pi i\beta\epsilon_0}, \quad 1 \leq n < N.$$

Setting

$$\mathbf{e} = \left[e_a\left(\frac{n + l_0}{N}T\right)\right]_{0 \leq n < 2n}, \quad \rho(m) = \rho\left(\frac{m}{N}T\right),\ 0 \leq m < N,$$

and

$$\mathbf{x}(\epsilon_0) = \begin{bmatrix} x_a^T(-\epsilon_0 + T) \\ x_a^T\left(-\epsilon_0 + \frac{1}{N}T\right) \\ \vdots \\ x_a^T\left(-\epsilon_0 + \frac{N-1}{N}T\right) \end{bmatrix} = w^{-2\pi i\beta\epsilon_0}\mathbf{x}, \quad \mathbf{x} = \mathbf{x}(0),$$

we have

$$\mathbf{e} = e^{-2\pi i\beta\epsilon_0}\frac{T}{N}\sum_{m=0}^{N-1}\rho(m)S_{2N}^{m+1}\left(S_N^{-1}\mathbf{x}\right)^{2N}$$

and

$$W_0P(2L,2)Z_{2L}\mathbf{e} = e^{-2\pi i\beta\epsilon_0}\frac{T}{N}\sum_{m=0}^{N-1}\rho(m)Z_LS_N^m\mathbf{x}.$$

Suppose a chirp x_j^T having carrier frequency β_j is transmitted from an antenna at $\mathbf{v}_j$ and interrogates dielectric materials having incident angle independent reflectivity kernels $\rho_a^{(j)}$ at $\mathbf{u}_i$, $0 \le i < I_0$. Set

$$u_{i,j} = \frac{2}{c}|\mathbf{v}_j - \mathbf{u}_i| = l_0\frac{T}{N} + \epsilon_{i,j},$$

where $l_0 \ge 0$ is an integer and $\epsilon_{i,j} < \frac{T}{N}$, $0 \le i < I_0$.

Setting

$$\mathbf{e}_j = \left[e_j\left(\frac{n+l_0}{N}T\right)\right]_{0\le n<2N},\quad \mathbf{x}_j = \left[x_j^T\left(\frac{n}{N}T\right)\right]_{0\le n<N}$$

and

$$\rho^{(i)}(m) = \rho_a^{(i)}\left(\frac{m}{N}T\right),\quad 0 \le m < N,$$

we have from the preceding discussion that

$$W_0P(2L,2)Z_{2L}\mathbf{e}_j = \frac{T}{N}\sum_{m=0}^{N-1}\left(\sum_{i=0}^{I_0-1}\rho^{(i)}(m)e^{-2\pi i\beta_ju_{i,j}}\right)Z_LS_N^m\mathbf{x}_j.$$

By orthogonality we compute

$$\Delta_j(m) = \sum_{i=0}^{I_0-1}\rho^{(i)}(m)e^{-2\pi i\beta_j\epsilon_{i,j}},\quad 0 \le m < N.$$

In matrix notation

$$[\Delta_j(m)]_{0\le m<N} = RE_j,$$

where R is the $N \times I_0$ matrix

$$R = \left[\rho^{(i)}(m)\right]_{0\le m<N,\,0\le i<I_0},$$

and E_j is the vector $\mathbf{C}^{I_0}$.

$$E_j = \left[e^{-2\pi i\beta_j\epsilon_{i,j}}\right]_{0\le i<I_0}.$$

Processing over J_0 antenna positions we compute

$$\Delta = RE,$$

where

$$\Delta = [\Delta_j(m)]_{0\le m<N,\,0\le j<J_0},$$

and

$$E = [E_0\ E_1\ \cdots\ E_{J_0-1}]\,.$$

E models the geometry of the measurements. In [1] we estimated R by pseudo-inversion of E and tested the accuracy of this inversion for several model geometry matrices E depending on the number of antenna positions J_0 the number of dielectric targets I_0, the spacing between antenna positions and the spacing between target positions.

Suppose that the reflectivity kernels depend on the incident angle. The $N \times I_0$ reflectivity kernel matrix R in the above discussion is replaced by J_0 $N \times I_0$ reflectivity kernel matrices

$$R(j), \quad 0 \leq j < J_0,$$

and we can compute by the above processing the J_0 vectors in $\mathbf{C}^N$

$$[\Delta_j(m)]_{0\leq m<N} = R(j)E_j, \quad 0 \leq j < J_0.$$

E_j is a vector in $\mathbf{C}^{I_0}$ depending on the carrier frequency of x_j and on the distances between antenna position $\mathbf{v}_j$ and I_0 dielectric targets.

We plan to develop algorithms for computing the matrix R_j by replacing the chirp pulse x_j by a sequence of chirp pulses at different carrier frequencies sufficiently separated in time such that the echo for each of the chirp pulses in the sequence can be independently measured and processed. This has the effect of replacing the vector E_j in $R(j)E_j$ by a $I_0 \times S$ matrix, S the number of chirp pulses in the sequence. The key to this approach is to choose the different carrier frequencies so that the pseudo-inversion of the resulting $I_0 \times S$ matrix will lead to a good estimate of $R(j)$.

The computation of $R(j)$ provides an estimate of the reflectivity kernels of the I_0 dielectric targets at incident angles determined by the geometric relationship between antenna position $\mathbf{v}_j$ and the I_0 dielectric targets. Processing over several antenna positions we get an incident angle dependent collection of reflectivity kernel estimates which we can compare with existing libraries.

In[1] we propose several models of incident angle dependence for the purpose of studying the effects of these models on algorithms for distinguishing a multiple dielectric target environment from multiple SAR measurements. For example if an antenna at

$$\mathbf{v} = (0, v, h)$$

transmits a pulse chirp which interrogates a dielectric target at

$$\mathbf{u} = (x, y, 0)$$

we assume that the dependence on the reflectivity kernel at $\mathbf{u}$ on incident angle could be expressed by

$$\rho_a\left(t, \frac{(x, 0, -h)}{|(x, 0, -h)|}\right).$$

In words the reflectivity kernel depends upon the slant direction and not on the broadside direction between target and antenna. The justification for this model is that the antenna footprint is relatively narrow in the along track direction so broadside variation is small.

The key to future work using this approach is to determine more realistic models of incident angle dependence and then to embed these models in algorithms.

In the preceding discussion we have not taken into account the possibility, even probability, that several dielectric targets are equidistant to given antenna position. If this is the case the algorithms described above compute the sum of reflectivity kernels of the equidistant targets. This is a standard SAR problem. An important part of a SAR algorithm package is usually devoted to distinguishing equidistant targets from one antenna position by utilizing measurements from other antenna positions. Although we have not included a discussion of this method, they will be an important part of the algorithmic development in this effort in SAR system algorithmic package.

16.4 Atmospheric effects

In this report we study the problem of removing the ionospheric effects from waveforms interrogating ground based dielectric material from a space-based radar by proposing two measurement strategies which in principle provide sufficient information to filter out the ionospheric effects by SVD methods. Unfortunately these methods can be highly fragile in noise.

We plan to study methods based more significantly on the electromagnetic properties of the atmosphere as a magnetically biased plasma and especially on the electromagnetic differences between this plasma and the interrogated dielectric material. Either combined with SVD framework or by themselves these differences will be the basis for constructing filters to remove ionospheric effects. We intend to study

- The Faraday rotation introduced by waveform propagating through a magnetically biased plasma (dielectric tensor).
- The model of magnetically biased plasma as a lossy dielectric whose electric susceptibility is negative [4] in distinction from a real dielectric material.
- The impulse response function for deterministic ionosphere as presented in [5].

Dr. Richard Albanese of Brooks City Base has shown that the echo resulting from wave propagation through a magnetically biased plasma followed by dielectric interrogation and returning through the plasma has a measurable Faraday rotation which (in most cases) is due solely to the plasma. Measurements of these Faraday rotations at several frequencies can be used to extract the electromagnetic properties of the plasma at transmission time. We intend to use this result to build an algorithm removing the ionospheric effects.

The deterministic ionospheric impulse response function depends upon electron density profiles. However so far these profiles cannot always be relied upon. We are most interested in the character of this impulse response function and not on its detailed expression. For example, we intend to use the fact that the time duration of this impulse response function is usually larger than the relaxation time of the dielectric material as a basis for removing deterministic ionospheric effects.

References

1. Phase II final technical report, contract # F33615–00–C–6012 30 April, 2002.

2. Myoung An and Richard Tolimieri, *Group Filters and Image Processing*, Psypher Press, 2003.

3. Guanghan Xu, Hui Liu, Lang Tong and Thomas Kailath, "A least-squares approach to blind channel identification," *IEEE Trans. SP* **43**(12), December 1995, 2982–2993.

4. Charles Herach Papas, *Theory of Electromagnetic Wave Propagation*, Dover 1965.

5. R.A. Roussel-Dupré and P. Argo, "Deterministic transfer function for transionospheric propagation," *Proc. Int. Beacon Sat. Symp.*, MIT Cambridge, 1992.

6. Richard Tolimieri and Myoung An, *Time-Frequency Representations*, Birkhauser, Boston 1998.

7. Richard Tolimieri, Myoung An and Chao Lu, *Algorithms for Fourier Transforms and Convolutions*, Springer-Verlag, 1997.